cancers

MDPI

*Article*

# Molecular Pathogenesis of Gene Regulation by the *miR-150* Duplex: *miR-150-3p* Regulates *TNS4* in Lung Adenocarcinoma

**Shunsuke Misono [1], Naohiko Seki [2,*], Keiko Mizuno [1], Yasutaka Yamada [2], Akifumi Uchida [1], Hiroki Sanada [1], Shogo Moriya [3], Naoko Kikkawa [2], Tomohiro Kumamoto [1], Takayuki Suetsugu [1] and Hiromasa Inoue [1]**

1 Department of Pulmonary Medicine, Graduate School of Medical and Dental Sciences, Kagoshima University, Kagoshima 890-8520, Japan; k8574402@kadai.jp (S.M.); keim@m.kufm.kagoshima-u.ac.jp (K.M.); akifumiuchida7883@gmail.com (A.U.); k8173956@kadai.jp (H.S.); kuma@m2.kufm.kagoshima-u.ac.jp (T.K.); taka3741@m2.kufm.kagoshima-u.ac.jp (T.S.); inoue-pulm@umin.net (H.I.)

2 Department of Functional Genomics, Graduate School of Medicine, Chiba University, Chuo-ku, Chiba 260-8670, Japan; yasutaka1205@olive.plala.or.jp (Y.Y.); naoko-k@hospital.chiba-u.jp (N.K.)

3 Department of Biochemistry and Genetics, Graduate School of Medicine, Chiba University, Chuo-ku, Chiba 260-8670, Japan; moriya.shogo@chiba-u.jp

* Correspondence: naoseki@faculty.chiba-u.jp; Tel.: +81-43-226-2971

Received: 6 March 2019; Accepted: 28 April 2019; Published: 30 April 2019


**Abstract:** Based on our miRNA expression signatures, we focused on *miR-150-5p* (the guide strand) and *miR-150-3p* (the passenger strand) to investigate their functional significance in lung adenocarcinoma (LUAD). Downregulation of *miR-150* duplex was confirmed in LUAD clinical specimens. In vitro assays revealed that ectopic expression of *miR-150-5p* and *miR-150-3p* inhibited cancer cell malignancy. We performed genome-wide gene expression analyses and in silico database searches to identify their oncogenic targets in LUAD cells. A total of 41 and 26 genes were identified as *miR-150-5p* and *miR-150-3p* targets, respectively, and they were closely involved in LUAD pathogenesis. Among the targets, we investigated the oncogenic roles of tensin 4 (*TNS4*) because high expression of *TNS4* was strongly related to poorer prognosis of LUAD patients (disease-free survival: $p = 0.0213$ and overall survival: $p = 0.0003$). Expression of *TNS4* was directly regulated by *miR-150-3p* in LUAD cells. Aberrant expression of TNS4 was detected in LUAD clinical specimens and its aberrant expression increased the aggressiveness of LUAD cells. Furthermore, we identified genes downstream from *TNS4* that were associated with critical regulators of genomic stability. Our approach (discovery of anti-tumor miRNAs and their target RNAs for LUAD) will contribute to the elucidation of molecular networks involved in the malignant transformation of LUAD.

**Keywords:** MicroRNA; *miR-150-5p*; *miR-150-3p*; lung adenocarcinoma; *TNS4*

## 1. Introduction

Lung cancer accounts for the largest number of cancer-related deaths in the world and its morbidity increases annually [1]. Lung adenocarcinoma (LUAD) is the most common histological subtype of non-small cell lung cancer (NSCLC) and this type of cancer is the leading cause of cancer-related deaths [2]. The survival rate of lung cancer has increased due to effective treatment strategies, including molecularly-targeted drugs and immune checkpoint inhibitors [3]. However, the efficacy of treatments for patients with distant metastases is limited, thereby resulting in poor prognosis [2]. In LUAD, metastasis occurs even if the primary tumor is small [4,5]. Therefore, the prognosis of advanced LUAD patients is poor, with average 5-year survival rates below 20% [6]. Therefore, additional research to

identify novel biomarkers for earlier detection and to develop effective targeted molecular therapies for LUAD is indispensable.

A vast number of studies have revealed that an extremely large number of non-coding RNAs are transcribed from the human genome and actually functional in various cellular processes. Among these non-coding RNAs, microRNAs (miRNAs) are endogenous single-stranded RNA molecules (19–22 nucleotides in length) that function as fine-tuners of RNA expression [7–11]. Importantly, a single miRNA can control a large number of RNA transcripts in normal and disease cells [7–11]. Recent studies showed that aberrant expression of miRNAs closely contributes to the pathogenesis of human diseases, including cancers via disruption of RNA networks [8–13].

We have been analyzing novel anti-tumor miRNA-mediated oncogenic targets and pathways that contribute to lung tumorigenesis [14–19]. Interestingly, our miRNA studies revealed that some passenger strands of miRNAs (e.g., *miR-144-5p* and *miR-145-3p*) derived from miRNA-duplex actually acted as anti-tumor miRNAs in lung squamous cell carcinoma [15,19]. More recently, we demonstrated that two miRNA species derived from *miR-145*-duplex (*miR-145-5p* and *miR-145-3p*) acted as anti-tumor miRNAs in LUAD via targeting several oncogenes [17].

Initially, it was thought that two types of miRNA were derived from double-stranded pre-miRNAs: guide strand miRNAs that control the target genes, and passenger strand miRNAs that lacked function and were degraded [20]. Our studies have altered the conventional understanding of miRNA biogenesis and have shown the importance of exploring passenger strands of miRNAs in cancer cells.

RNA sequencing-based miRNA expression signatures contribute to a new development of molecular pathogenesis of human cancers. miRNA expression signatures in human cancers revealed that two miRNAs derived from *miR-150*-duplex—*miR-150-5p* (the guide strand) and *miR-150-3p* (the passenger strand)—are frequently downregulated in several types of cancers [21–23]. Reports of *miR-150-5p* in cancers are scattered across public databases, but there are few reports of *miR-150-3p*. We have analyzed the anti-tumor activity of *miR-150-3p* in esophageal and head and neck squamous cell carcinomas [22,23]. With regard to LUAD, no such reports are available, and this is an important facet of the functional analysis of *miR-150-3p* and the search for target genes.

The aim of this study was to investigate the anti-tumor roles of both strands of *miR-150*-duplex and to identify their targets with close associations with LUAD tumorigenesis. The Cancer Genome Atlas (TCGA) revealed that low expression of *miR-150-5p* and *miR-150-3p* predicted poor prognosis. Ectopic expression of two miRNAs significantly attenuated the malignant phenotypes of cancer cells. Moreover, we identified several oncogenic targets by *miR-150-3p* regulation in LUAD cells.

## 2. Results

### *2.1. miR-150-5p and miR-150-3p were Downregulated in Lung Adenocarcinoma (LUAD) Specimens and Cell Lines*

To explore whether *miR-150-5p* and *miR-150-3p* are downregulated in LUAD, expression levels of *miR-150-5p* and *miR-150-3p* in clinical specimens were measured. The characteristics of the patients are recorded in Table 1.

We found that expression of the *miR-150* duplex was significantly decreased in LUAD specimens and LUAD cell lines relative to non-cancerous tissues ($p = 0.0078$ and $p < 0.0001$, respectively, Figure 1A,B). There were positive correlations between the expression levels of *miR-150-5p* and *miR-150-3p* by Spearman's rank test ($r = 0.7156$ and $p < 0.0001$, Figure 1C). According to the Kaplan–Meier overall survival curves using TCGA database, we found that the low expression levels of *miR-150-5p* and *miR-150-3p* were associated with poor prognosis in LUAD patients (overall survival, $p = 0.0078$ and $p = 0.0435$, respectively, Figure 1D,E).

**Table 1.** Characteristics of lung cancer and non-cancerous cases.

| **A. Characteristics of the Lung Cancer Cases** | | |
|---|---|---|
| **Lung Cancer Patients** | **n** | **(%)** |
| Total number | 18 | |
| Median age (range) | 73.5 (59–86) | |
| Gender | | |
| Male | 9 | 50.0 |
| Female | 9 | 50.0 |
| Pathological stage: | | |
| IA | 1 | 5.6 |
| IB | 4 | 22.2 |
| IIA | 8 | 44.4 |
| IIB | 1 | 5.6 |
| IIIA | 4 | 22.2 |
| IIIB | 0 | 0.0 |
| **B. Characteristics of the Non-Cancerous Cases** | | |
| **Non-Cancerous Tissues** | **n** | **(%)** |
| Total number | 28 | |
| Median age (range) | 71 (50–88) | |
| Gender: | | |
| Male | 25 | 89.3 |
| Female | 3 | 10.7 |

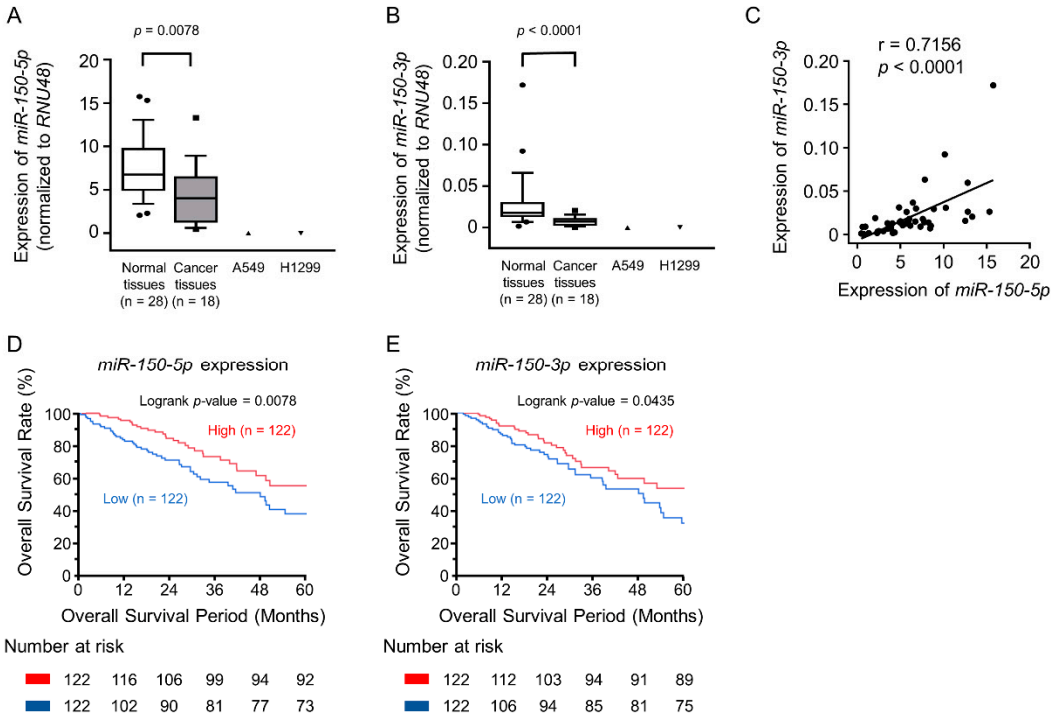


**Figure 1.** The clinical significance of *miR-150-5p* and *miR-150-3p* expression in lung adenocarcinoma (LUAD). (**A**,**B**) Downregulation of *miR-150-5p* and *miR-150-3p* expression in clinical specimens of LUAD and two cell lines (A549 and H1299). Expression of *RNU48* was used as an internal control. (**C**) Expression of two miRNAs derived from *miR-150*-duplex were positive correlation by Spearman's rank test. (**D**,**E**) The Kaplan–Meier overall survival curve analyses of patients with LUAD by The Cancer Genome Atlas (TCGA) database. Patients were divided into two groups according to miRNA expression and analyzed.

### 2.2. Overexpression of miR-150-5p and miR-150-3p Inhibits Cancer Cell Aggressiveness

To investigate the biological functions of *miR-150-5p* and *miR-150-3p* in LUAD, we performed gain-of-function assays using miRNA transfection into LUAD cell lines (A549 and H1299). Cell proliferation assays showed that *miR-150-5p*- and *miR-150-3p*- transfected LUAD cells had reduced cell growth compared with mock- or miR-control-transfected LUAD cells (Figure 2A). Also, cell migratory and invasive abilities were markedly decreased in the LUAD cells transfected with *miR-150-5p* and *miR-150-3p* (Figure 2B,C).

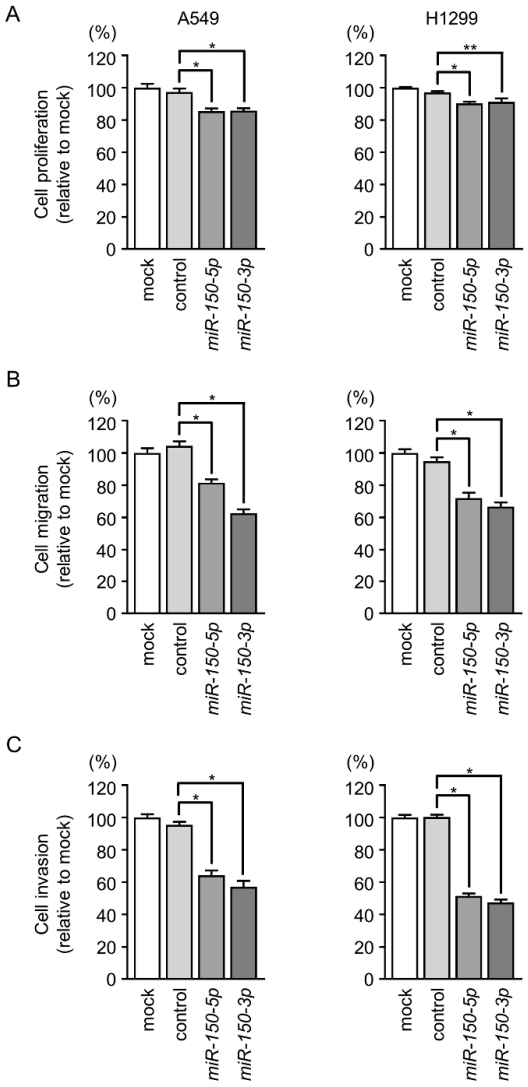


**Figure 2.** Functional assays of *miR-150-5p* and *miR-150-3p* in LUAD cells (A549 and H1299). (**A**–**C**) Cell proliferation, migration, and invasive activities were significantly blocked by ectopic expression of *miR-150-5p* or *miR-150-3p*. * $p < 0.01$, ** $p < 0.05$.

Furthermore, we performed functional analysis by reducing the concentration of *miR-150-3p* (1 nM and 0.1 nM) transfection into LUAD cells. Our data showed that antitumor functions (inhibition of cancer cell proliferation, migration, and invasion) were observed at 1 nM concentration, although there were no antitumor functions at 0.1 nM concentration on A549 and H1299 cells (Figure S1).

### *2.3. Incorporation of miR-150-5p and miR-150-3p into the RNA-induced silencing complex (RISC) in LUAD Cells*

We next performed immunoprecipitation with antibodies targeting Ago2, which plays a pivotal role in the uptake of miRNAs into the RISC (Figure S2A). After transfection of A549 cells with *miR-150-5p* and immunoprecipitation by anti-Ago2 antibodies, *miR-150-5p* levels in the immunoprecipitates were significantly higher than those of mock- or miR-control-transfected cells and those of *miR-150-3p*-transfected cells ($p < 0.01$; Figure S2B–D). Similarly, after *miR-150-3p* transfection (10 nM, 1 nM, and 0.1 nM), substantial amounts of *miR-150-3p* were detected in Ago2 immunoprecipitates ($p < 0.01$; Figure S2B–D).

### *2.4. Candidate Target Genes of miR-150-5p and miR-150-3p Regulation in LUAD: Clinical Significance of TNS4, SFXN1, SKA3, and SPOCK1 Expression*

Our selection strategy of *miR-150-5p*- and *miR-150-3p*-regulated oncogenic targets is shown in Figure S3A,B. A total of 41 and 26 oncogenic targets regulated by *miR-150-5p* and *miR-150-3p* were identified in LUAD cells (Tables 2 and 3).

**Table 2.** Candidate target genes regulated by *miR-150-5p.*

| Entrez Gene | Gene Symbol | Gene Name | Total Sites | A549 *miR-150-5p* Transfectant FC ($log_2$) | GSE19188 FC ($log_2$) | TCGA OncoLnc *p*-Value |
|---|---|---|---|---|---|---|
| 4751 | *NEK2* | NIMA-related kinase 2 | 1 | −0.565 | 3.323 | <0.0001 |
| 64065 | *PERP* | PERP, TP53 apoptosis effector | 3 | −3.012 | 1.835 | <0.0001 |
| 5122 | *PCSK1* | Proprotein convertase subtilisin/kexin type 1 | 1 | −0.680 | 2.532 | 0.0006 |
| 84985 | *FAM83A* | Family with sequence similarity 83, member A | 1 | −0.717 | 3.188 | 0.0010 |
| 1033 | *CDKN3* | Cyclin-dependent kinase inhibitor 3 | 2 | −0.582 | 2.889 | 0.0011 |
| 6241 | *RRM2* | Ribonucleotide reductase M2 | 3 | −2.433 | 3.000 | 0.0013 |
| 79801 | *SHCBP1* | SHC SH2-domain binding protein 1 | 1 | −1.118 | 1.841 | 0.0015 |
| 29127 | *RACGAP1* | Rac GTPase activating protein 1 | 2 | −0.545 | 1.677 | 0.0019 |
| 24137 | *KIF4A* | Kinesin family member 4A | 1 | −0.933 | 3.309 | 0.0030 |
| 6695 | *SPOCK1* | Pparc/osteonectin, cwcv and kazal-like domains proteoglycan (testican) 1 | 1 | −0.764 | 1.696 | 0.0031 |
| 9837 | *GINS1* | GINS complex subunit 1 (Psf1 homolog) | 2 | −0.749 | 2.991 | 0.0076 |
| 339761 | *CYP27C1* | Cytochrome P450, family 27, subfamily C, polypeptide 1 | 4 | −2.360 | 1.706 | 0.0126 |
| 10331 | *B3GNT3* | UDP-GlcNAc:betaGal beta-1,3-N-acetylglucosaminyltransferase 3 | 2 | −0.939 | 1.608 | 0.0129 |
| 79962 | *DNAJC22* | DnaJ (Hsp40) homolog, subfamily C, member 22 | 5 | −0.908 | 2.031 | 0.0201 |
| 10635 | *RAD51AP1* | RAD51-associated protein 1 | 1 | −0.611 | 2.470 | 0.0228 |
| 10797 | *MTHFD2* | Methylenetetrahydrofolate dehydrogenase (NADP+ dependent) 2, methenyltetrahydrofolate cyclohydrolase | 1 | −1.905 | 1.887 | 0.0236 |
| 9699 | *RIMS2* | Regulating synaptic membrane exocytosis 2 | 2 | −0.697 | 1.976 | 0.0265 |
| 1058 | *CENPA* | Centromere protein A | 1 | −1.019 | 3.488 | 0.0365 |
| 23657 | *SLC7A11* | Solute carrier family 7 (anionic amino acid transporter light chain, xc- system), member 11 | 3 | −1.093 | 2.014 | 0.0474 |
| 3755 | *KCNG1* | Potassium voltage-gated channel, subfamily G, member 1 | 5 | −1.069 | 1.887 | 0.0557 |
| 1825 | *DSC3* | Desmocollin 3 | 1 | −1.247 | 2.488 | 0.0667 |
| 388228 | *SBK1* | SH3 domain binding kinase 1 | 1 | −0.658 | 1.745 | 0.0939 |
| 8038 | *ADAM12* | ADAM metallopeptidase domain 12 | 2 | −0.668 | 2.753 | 0.1097 |
| 84733 | *CBX2* | Chromobox homolog 2 | 1 | −0.591 | 1.988 | 0.1116 |
| 130827 | *TMEM182* | Transmembrane protein 182 | 1 | −0.690 | 1.568 | 0.1189 |
| 92312 | *MEX3A* | mex-3 RNA binding family member A | 3 | −0.584 | 1.986 | 0.1271 |
| 4323 | *MMP14* | Matrix metallopeptidase 14 | 3 | −0.621 | 1.872 | 0.1296 |
| 4151 | *MB* | myoglobin | 3 | −1.119 | 1.614 | 0.1346 |
| 57167 | *SALL4* | Sal-like 4 (Drosophila) | 1 | −0.582 | 2.836 | 0.2382 |
| 256714 | *MAP7D2* | MAP7 domain containing 2 | 1 | −1.449 | 2.007 | 0.2798 |
| 6273 | *S100A2* | S100 calcium binding protein A2 | 1 | −0.643 | 2.513 | 0.3132 |
| 200844 | *C3orf67* | Chromosome 3 open reading frame 67 | 1 | −0.514 | 1.584 | 0.3482 |
| 1690 | *COCH* | Cochlin | 2 | −0.592 | 3.406 | 0.3696 |
| 10447 | *FAM3C* | Family with sequence similarity 3, member C | 1 | −1.570 | 1.536 | 0.3847 |
| 147920 | *IGFL2* | IGF-like family member 2 | 1 | −0.719 | 2.569 | 0.4596 |
| 547 | *KIF1A* | Kinesin family member 1A | 4 | −0.733 | 2.518 | 0.6354 |
| 9066 | *SYT7* | Synaptotagmin VII | 2 | −0.921 | 1.730 | 0.7141 |
| 55220 | *KLHDC8A* | Kelch domain containing 8A | 4 | −1.168 | 1.709 | 0.7484 |
| 440590 | *ZYG11A* | Zyg-11 family member A, cell cycle regulator | 2 | −1.619 | 1.826 | 0.7530 |
| 3141 | *HLCS* | Holocarboxylase synthetase | 1 | −0.897 | 1.791 | 0.8947 |
| 9547 | *CXCL14* | Chemokine (C-X-C motif) ligand 14 | 2 | −0.750 | 1.800 | 0.9229 |

**Table 3.** Candidate target genes regulated by *miR-150-3p*.

| Entrez Gene | Gene Symbol | Gene Name | Total Sites | A549 *miR-150-3p* Transfectant FC ($log_2$) | GSE19188 FC ($log_2$) | TCGA OncoLnc *p*-Value |
|---|---|---|---|---|---|---|
| 84951 | *TNS4* | Tensin 4 | 1 | −1.318 | 2.560 | 0.0003 |
| 94081 | *SFXN1* | Sideroflexin 1 | 1 | −1.307 | 1.404 | 0.0020 |
| 221150 | *SKA3* | Spindle and kinetochore-associated complex subunit 3 | 1 | −1.006 | 2.015 | 0.0027 |
| 6695 | *SPOCK1* | Sparc/osteonectin, cwcv and kazal-like domains proteoglycan (testican) 1 | 3 | −2.040 | 1.696 | 0.0031 |
| 89874 | *SLC25A21* | Solute carrier family 25 (mitochondrial oxoadipate carrier), member 21 | 2 | −2.557 | 1.358 | 0.0149 |
| 94032 | *CAMK2N2* | Calcium/calmodulin-dependent protein kinase II inhibitor 2 | 1 | −1.303 | 1.538 | 0.0208 |
| 5738 | *PTGFRN* | Prostaglandin F2 receptor inhibitor | 2 | −1.750 | 1.237 | 0.0291 |
| 23105 | *FSTL4* | Follistatin-like 4 | 1 | −1.602 | 1.485 | 0.0589 |
| 130574 | *LYPD6* | LY6/PLAUR domain containing 6 | 1 | −1.004 | 1.917 | 0.0591 |
| 150223 | *YDJC* | YdjC homolog (bacterial) | 1 | −1.592 | 1.088 | 0.0699 |
| 3174 | *HNF4G* | Hepatocyte nuclear factor 4, gamma | 1 | −1.827 | 1.709 | 0.0717 |
| 6857 | *SYT1* | Synaptotagmin I | 1 | −2.264 | 2.058 | 0.0735 |
| 5522 | *PPP2R2C* | Protein phosphatase 2, regulatory subunit B, gamma | 2 | −1.004 | 2.491 | 0.1067 |
| 8038 | *ADAM12* | ADAM metallopeptidase domain 12 | 2 | −1.555 | 2.753 | 0.1097 |
| 84216 | *TMEM117* | Transmembrane protein 117 | 1 | −3.167 | 1.049 | 0.1894 |
| 55753 | *OGDHL* | Oxoglutarate dehydrogenase-like | 1 | −1.896 | 1.776 | 0.3167 |
| 79944 | *L2HGDH* | L-2-hydroxyglutarate dehydrogenase | 1 | −1.921 | 1.730 | 0.3221 |
| 79776 | *ZFHX4* | Zinc finger homeobox 4 | 1 | −2.113 | 1.248 | 0.3578 |
| 4647 | *MYO7A* | Myosin VIIA | 1 | −1.193 | 1.047 | 0.4080 |
| 23321 | *TRIM2* | Tripartite motif containing 2 | 2 | −1.550 | 1.755 | 0.4560 |
| 401474 | *SAMD12* | Sterile alpha motif domain containing 12 | 1 | −1.950 | 1.027 | 0.4853 |
| 145282 | *MIPOL1* | Mirror-image polydactyly 1 | 1 | −1.401 | 1.108 | 0.5861 |
| 8821 | *INPP4B* | Inositol polyphosphate-4-phosphatase, type II, 105kDa | 3 | −1.412 | 1.414 | 0.6077 |
| 80310 | *PDGFD* | Platelet-derived growth factor D | 1 | −1.555 | 1.142 | 0.6859 |
| 9802 | *DAZAP2* | DAZ-associated protein 2 | 2 | −1.439 | 1.144 | 0.8241 |
| 85439 | *STON2* | Stonin 2 | 1 | −1.371 | 1.079 | 0.9773 |

In this study, we focused on *miR-150-3p*, which is the passenger strand of the *miR-150* duplex and had pronounced anti-tumor function. We examined the relation between the pathogenesis of LUAD and these targets using TCGA database and found four genes (*TNS4*, *SFXN1*, *SKA3*, *SPOCK1*) that were strongly associated with patient outcomes (5-year overall survival, $p < 0.01$, Figure 3A–D). Finally, we focused on *TNS4*, the expression of which was strongly associated with poor prognosis of LUAD patients (disease-free survival: $p = 0.0213$ and overall survival: $p = 0.0003$) among the four genes and validated the effect on LUAD cells.

### 2.5. *miR-150-3p Directly Regulated TNS4 in A549 Cells*

In cells transfected with *miR-150-3p*, the levels of *TNS4* mRNA and TNS4 protein were significantly lower than mock- or miR-control-transfected cells (Figure 4A,B). Furthermore, the expression of *TNS4* mRNA and TNS4 protein was suppressed at the diluted concentration of *miR-150-3p* precursor (1 nM and 0.1 nM) (Figure S4A,B).

In order to confirm the binding site of *miR-150-3p*, the nucleotide sequences of 3'UTR (UTR: untranslated region) of *TNS4* in A549 cells was examined independently. Our data showed that several variants of the 3'UTR of *TNS4* existed in A549 cells (Figure S5). As a result of sequencing analyses, one putative binding site of the *miR-150-3p* was found in 3'UTR of *TNS4* (Figure S5). Based on our sequence data, we used luciferase reporter assays with vectors carrying either the wild-type or deletion-type 3'-UTR of *TNS4* (Figure 4C). We observed significantly reduced luminescence intensities after transfection with *miR-150-3p* and the wild-type 3'-UTR of *TNS4* (Figure 4C). Transfection with the deletion-type vector did not reduced luminescence intensities in A549 cells (Figure 4C). Thus, *miR-150-3p* directly bound to *TNS4* in the 3'-UTR. Although TargetScanHuman database predicted putative binding sites of *miR-150-5p* in 3'UTR of *TNS4*, our sequencing data could not confirm the sequences.

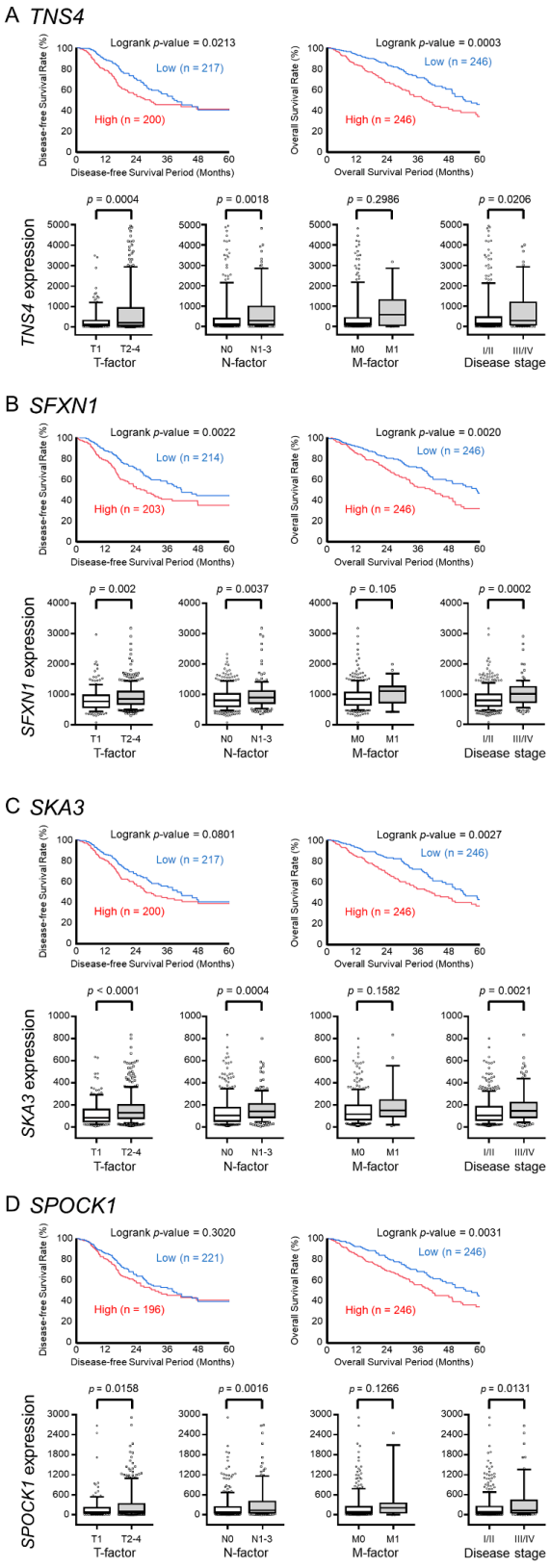


**Figure 3.** The relationship between the expression levels of four genes (*TNS4*, *SFXN1*, *SKA3*, and *SPOCK1*) and clinical significance based on The Cancer Genome Atlas (TCGA) database. (**A**–**D**) The Kaplan–Meier disease-free survival curves and overall survival curves, T factor, N factor, M factor, and disease stage of the high- and low-expression groups for four genes (*TNS4*, *SFXN1*, *SKA3*, and *SPOCK1*).

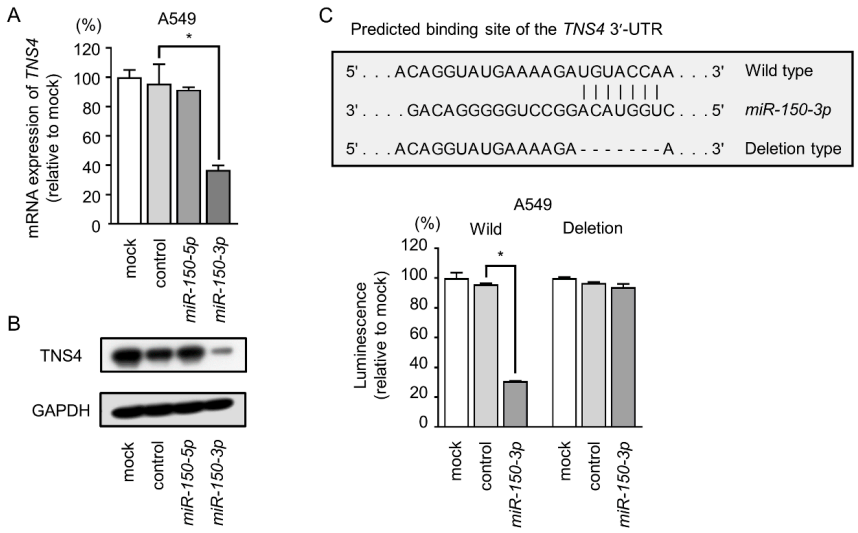


**Figure 4.** *TNS4* was directly controlled by *miR-150-3p* in LUAD cells. (**A**,**B**) *TNS4* mRNA and protein expression was reduced by *miR-150-3p* ectopic expression (48 h after transfection). *GUSB* was used as an expression control. GAPDH was used as a loading control. * $p < 0.01$. (**C**) Dual luciferase reporter assays using vectors encoding the wild-type *TNS4* 3′-UTR sequence containing one putative *miR-150-3p* target site (wild) and 3′-UTR sequences with deletions of the target site (deletion). Normalized data were calculated as the ratio of *Renilla*/firefly luciferase activities. * $p < 0.01$. UTR: untranslated region.

## 2.6. Expression of TNS4 Protein in Clinical LUAD Specimens

Analysis using a tissue microarray was performed to examine TNS4 expression at the protein level. We validated the expression of TNS4 by using immunohistochemical staining. In this study, we stained 20 LUAD specimens and 14 non-cancerous specimens. Clinical information on the tissue microarray is shown in the Table S2. Compared with non-cancerous tissues, TNS4 proteins were highly expressed in LUAD specimens (Figure 5).

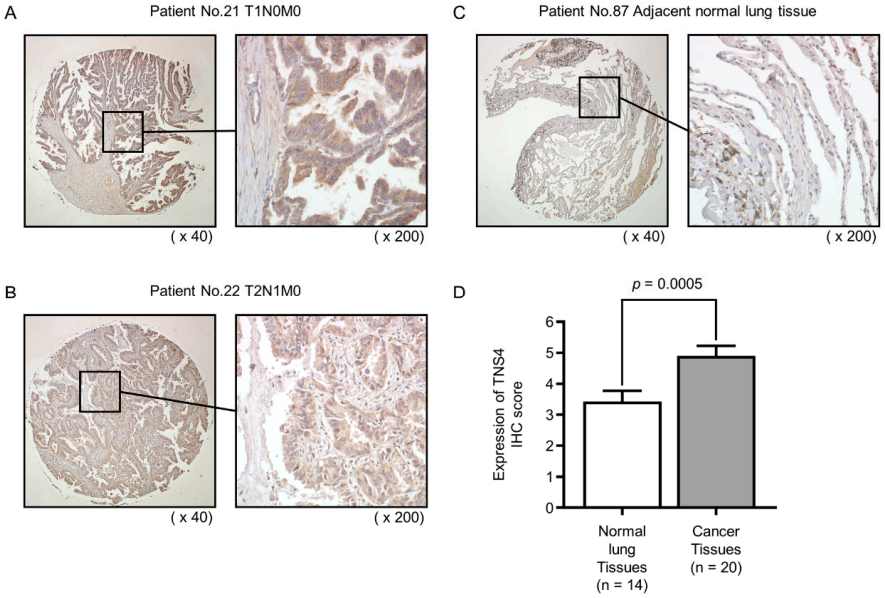


**Figure 5.** Immunohistochemical staining of TNS4 protein in clinical LUAD specimens. (**A**,**B**) The overexpression of TNS4 was observed in the cytoplasm of cancer cells. (**C**) TNS4 was weakly stained or not detected in normal lung specimens. (**D**) Comparison of immunohistochemical staining of TNS4 in LUAD specimens and normal lung specimens. LUAD specimens showed higher expression of TNS4 than normal lung specimens.

### 2.7. TNS4 Silencing Suppresses the Aggressiveness of LUAD Cells

To confirm the effect of *TNS4* on LUAD cells, we used si-*TNS4* to knock down its expression in A549 cells. RT-PCR and Western blotting showed that expression levels of both *TNS4* mRNA and TNS4 protein were markedly reduced by both si-*TNS4*-1 and si-*TNS4*-2 (Figure 6A,B). In functional assays, cell proliferation, migration, and invasive abilities were significantly suppressed by si-*TNS4* transfection in LUAD cells (Figure 6C–E).

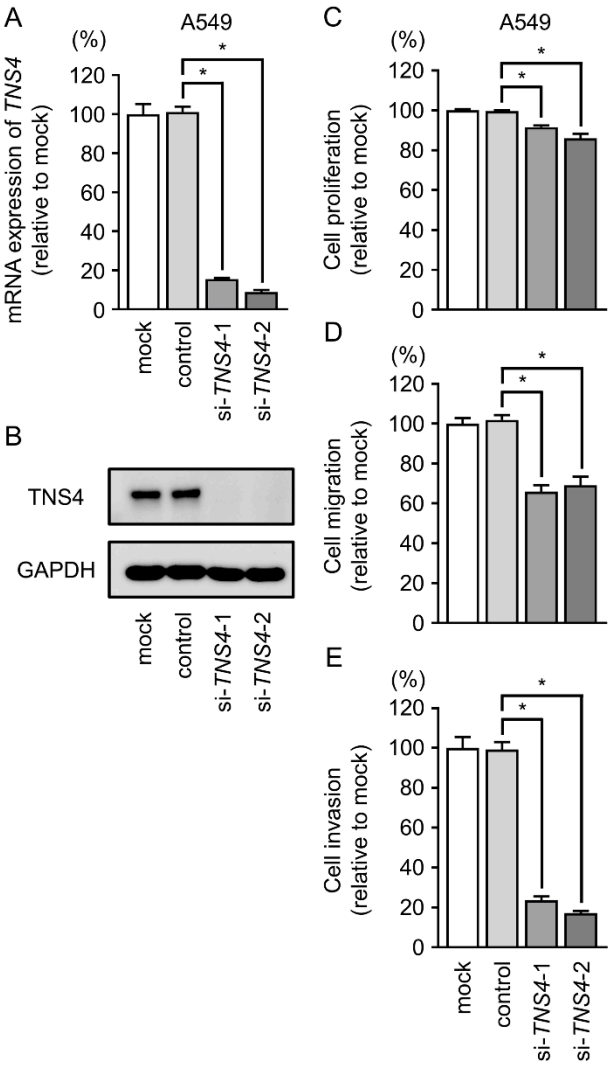


**Figure 6.** Knockdown studies of *TNS4*/TNS4 using si-*TNS4* in LUAD cells (A549 and H1299). (**A**,**B**) *TNS4* mRNA and protein expression 48 h after transfection of si-*TNS4*-1 or si-*TNS4*-2 in LUAD cell lines. (**C**–**E**) Cell proliferation, migration, and invasive activities were significantly blocked by si-*TNS4* transfection into LUAD cell lines. * $p < 0.01$.

### 2.8. Gain-of-Function Studies by TNS4 Expression Vector

To explore whether *TNS4* promoted cell proliferation, migration, and invasive abilities, we transfected pCMV-*TNS4* into H1299 cells and performed functional assays. Western blotting indicated that overexpression of TNS4 protein was observed in pCMV-*TNS4* vector-transfected cells (Figure 7A). Furthermore, cell migration and invasion were significantly enhanced in pCMV-*TNS4* vector-transfected cells (Figure 7B–D).

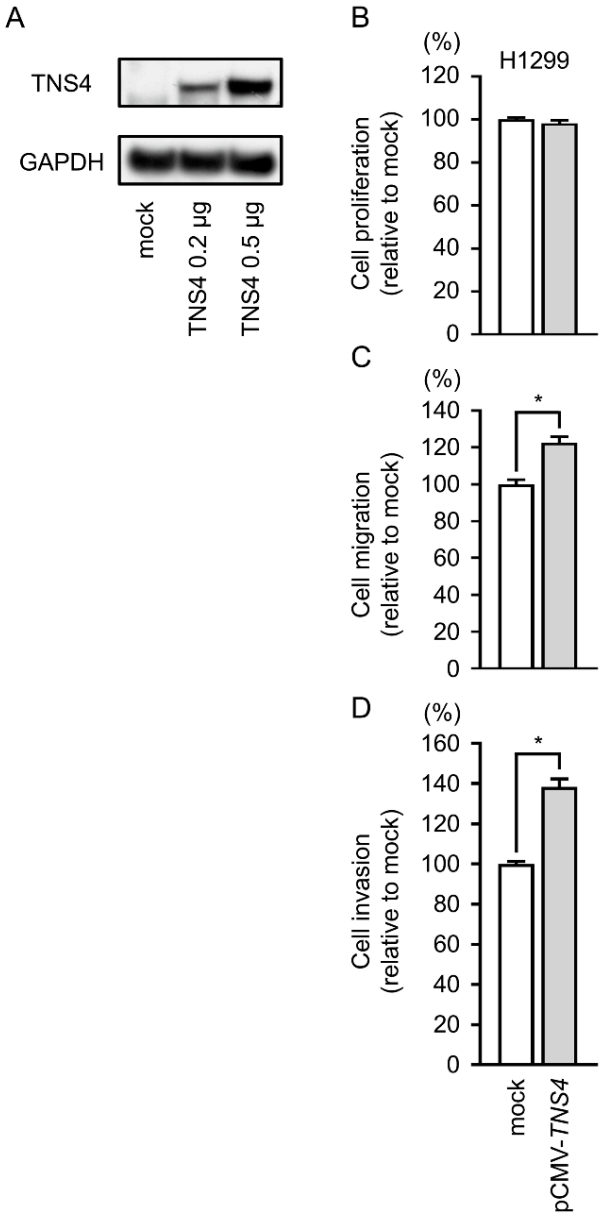


**Figure 7.** The effects of *TNS4* overexpression by H1299 cells. (**A**) Expression levels of TNS4 protein 48 h after transfection with pCMV-*TNS4* vector into H1299 cells. (**B**) Cell proliferation was evaluated by XTT assays. (**C**) Cell migration was determined by wound healing assay 24 h after forward transfection with the pCMV-*TNS4* vector. (**D**) Cell invasion was determined by Matrigel assay 24 h after forward transfection with the pCMV-*TNS4* vector. These assays showed that migratory and invasive activities were increased in pCMV-*TNS4* vector-transfected cell lines. * $p < 0.01$.

### *2.9. Downstream Genes Affected by the Silencing of TNS4 in LUAD Cells*

We performed genome-wide gene expression analysis in LUAD cells transfected with si-*TNS4* and in silico analysis to investigate the downstream genes regulated by *TNS4*. A total of 1521 downregulated genes were identified using gene expression analysis in LUAD cells transfected with si-*TNS4*. Among them, we found high expression of genes in the NSCLC clinical expression profiles from the GEO database (GEO accession no: GSE 19188). A total of 88 genes were identified as *TNS4*-modulated genes (Table 4 and Figure S6).

**Table 4.** Candidate downstream genes modulated by *TNS4* in lung adenocarcinoma.

| Entrez Gene | Gene Symbol | Gene Name | GSE19188 FC ($log_2$) | A549 si-*TNS4*-2 Transfectant FC ($log_2$) | TCGA OncoLnc *p*-Value |
|---|---|---|---|---|---|
| 114904 | *C1QTNF6* | C1q and tumor necrosis factor related protein 6 | 2.046 | −1.159 | <0.0001 |
| 983 | *CDK1* | Cyclin-dependent kinase 1 | 2.400 | −1.119 | 0.0003 |
| 10615 | *SPAG5* | Sperm-associated antigen 5 | 2.196 | −1.598 | 0.0003 |
| 84951 | *TNS4* | Tensin 4 | 2.560 | −2.690 | 0.0003 |
| 4288 | *MKI67* | Marker of proliferation Ki-67 | 2.835 | −1.475 | 0.0004 |
| 8208 | *CHAF1B* | Chromatin assembly factor 1, subunit B (p60) | 1.723 | −1.112 | 0.0005 |
| 9824 | *ARHGAP11A* | Rho GTPase activating protein 11A | 1.638 | −1.263 | 0.0007 |
| 9055 | *PRC1* | Protein regulator of cytokinesis 1 | 2.540 | −1.120 | 0.0007 |
| 171177 | *RHOV* | Ras homolog family member V | 2.330 | −1.890 | 0.0008 |
| 1033 | *CDKN3* | Cyclin-dependent kinase inhibitor 3 | 2.889 | −1.594 | 0.0011 |
| 6241 | *RRM2* | Ribonucleotide reductase M2 | 3.000 | −1.356 | 0.0013 |
| 57405 | *SPC25* | SPC25, NDC80 kinetochore complex component | 2.417 | −1.456 | 0.0014 |
| 5318 | *PKP2* | Plakophilin 2 | 1.584 | −1.108 | 0.0016 |
| 701 | *BUB1B* | BUB1 mitotic checkpoint serine/threonine kinase B | 2.669 | −1.278 | 0.0017 |
| 4085 | *MAD2L1* | MAD2 mitotic arrest deficient-like 1 (yeast) | 2.768 | −1.726 | 0.0018 |
| 81624 | *DIAPH3* | Diaphanous-related formin 3 | 1.926 | −1.016 | 0.0022 |
| 3832 | *KIF11* | Kinesin family member 11 | 2.479 | −1.007 | 0.0022 |
| 79019 | *CENPM* | Centromere protein M | 2.391 | −1.057 | 0.0023 |
| 55635 | *DEPDC1* | DEP domain containing 1 | 3.443 | −1.282 | 0.0024 |
| 147841 | *SPC24* | SPC24, NDC80 kinetochore complex component | 2.179 | −1.490 | 0.0031 |
| 195828 | *ZNF367* | Zinc finger protein 367 | 1.583 | −1.454 | 0.0033 |
| 1063 | *CENPF* | Centromere protein F, 350/400kDa | 2.985 | −1.129 | 0.0048 |
| 83540 | *NUF2* | NUF2, NDC80 kinetochore complex component | 3.442 | −1.069 | 0.0048 |
| 29089 | *UBE2T* | Ubiquitin-conjugating enzyme E2T | 3.317 | −1.092 | 0.0051 |
| 7348 | *UPK1B* | Uroplakin 1B | 1.603 | −1.179 | 0.0059 |
| 11130 | *ZWINT* | ZW10 interacting kinetochore protein | 2.184 | −1.188 | 0.0064 |
| 11169 | *WDHD1* | WD repeat and HMG-box DNA binding protein 1 | 2.094 | −1.151 | 0.0065 |
| 55215 | *FANCI* | Fanconi anemia, complementation group I | 2.298 | −1.563 | 0.0073 |
| 4176 | *MCM7* | Minichromosome maintenance complex component 7 | 1.555 | −1.164 | 0.0076 |
| 10403 | *NDC80* | NDC80 kinetochore complex component | 2.493 | −1.053 | 0.0076 |
| 699 | *BUB1* | BUB1 mitotic checkpoint serine/threonine kinase | 3.206 | −1.180 | 0.0081 |
| 79075 | *DSCC1* | DNA replication and sister chromatid cohesion 1 | 1.704 | −1.187 | 0.0088 |
| 51514 | *DTL* | Denticleless E3 ubiquitin protein ligase homolog (Drosophila) | 2.098 | −1.187 | 0.0091 |
| 8914 | *TIMELESS* | Timeless circadian clock | 1.650 | −1.447 | 0.0093 |
| 79733 | *E2F8* | E2F transcription factor 8 | 2.879 | −2.313 | 0.0114 |
| 4605 | *MYBL2* | v-Myb avian myeloblastosis viral oncogene homolog-like 2 | 3.003 | −1.063 | 0.0122 |
| 5427 | *POLE2* | Polymerase (DNA directed), epsilon 2, accessory subunit | 1.600 | −1.074 | 0.0122 |
| 10331 | *B3GNT3* | UDP-GlcNAc:betaGal beta-1,3-N-acetylglucosaminyltransferase 3 | 1.608 | −1.005 | 0.0129 |
| 7083 | *TK1* | Thymidine kinase 1, soluble | 2.086 | −1.399 | 0.0131 |
| 6790 | *AURKA* | Aurora kinase A | 2.542 | −1.018 | 0.0132 |
| 79623 | *GALNT14* | Polypeptide N-acetylgalactosaminyltransferase 14 | 2.572 | −1.075 | 0.0140 |
| 64151 | *NCAPG* | Non-SMC condensin I complex, subunit G | 2.833 | −2.675 | 0.0147 |
| 8318 | *CDC45* | Cell division cycle 45 | 3.829 | −1.605 | 0.0159 |
| 55165 | *CEP55* | Centrosomal protein 55kDa | 2.875 | −1.077 | 0.0203 |
| 54478 | *FAM64A* | Family with sequence similarity 64, member A | 2.713 | −1.697 | 0.0219 |
| 79172 | *CENPO* | Centromere protein O | 1.620 | −1.048 | 0.0248 |
| 2491 | *CENPI* | Centromere protein I | 2.088 | −1.685 | 0.0258 |
| 1356 | *CP* | Ceruloplasmin (ferroxidase) | 1.604 | −2.134 | 0.0300 |
| 2244 | *FGB* | Fibrinogen beta chain | 1.887 | −3.066 | 0.0305 |
| 29128 | *UHRF1* | Ubiquitin-like with PHD and ring finger domains 1 | 2.576 | −1.442 | 0.0312 |
| 1058 | *CENPA* | Centromere protein A | 3.488 | −1.338 | 0.0365 |
| 2877 | *GPX2* | Glutathione peroxidase 2 (gastrointestinal) | 3.579 | −1.038 | 0.0446 |
| 5888 | *RAD51* | RAD51 recombinase | 2.085 | −1.344 | 0.0478 |
| 8438 | *RAD54L* | RAD54-like (S. cerevisiae) | 2.920 | −1.013 | 0.0509 |
| 1789 | *DNMT3B* | DNA (cytosine-5-)-methyltransferase 3 beta | 1.606 | −1.029 | 0.0607 |
| 5984 | *RFC4* | Replication factor C (activator 1) 4, 37kDa | 2.004 | −1.166 | 0.0938 |
| 91057 | *CCDC34* | Coiled-coil domain containing 34 | 1.995 | −1.985 | 0.1035 |
| 202915 | *TMEM184A* | Transmembrane protein 184A | 1.940 | −1.983 | 0.1067 |
| 8038 | *ADAM12* | ADAM metallopeptidase domain 12 | 2.753 | −1.464 | 0.1097 |
| 51557 | *LGSN* | Lengsin, lens protein with glutamine synthetase domain | 1.721 | −1.008 | 0.1253 |
| 4151 | *MB* | Myoglobin | 1.614 | −2.307 | 0.1346 |
| 201299 | *RDM1* | RAD52 motif containing 1 | 1.503 | −1.596 | 0.1583 |
| 5080 | *PAX6* | Paired box 6 | 1.602 | −1.692 | 0.1649 |
| 114907 | *FBXO32* | F-box protein 32 | 1.990 | −1.044 | 0.1654 |
| 286151 | *FBXO43* | F-box protein 43 | 1.569 | −1.906 | 0.1729 |
| 10293 | *TRAIP* | TRAF interacting protein | 2.362 | −1.114 | 0.1742 |
| 83990 | *BRIP1* | BRCA1 interacting protein C-terminal helicase 1 | 2.051 | −1.439 | 0.1829 |
| 349136 | *WDR86* | WD repeat domain 86 | 1.653 | −1.306 | 0.1904 |
| 1870 | *E2F2* | E2F transcription factor 2 | 1.704 | −1.075 | 0.1993 |
| 3007 | *HIST1H1D* | Histone cluster 1, H1d | 1.568 | −1.265 | 0.2918 |
| 6676 | *SPAG4* | Sperm-associated antigen 4 | 1.552 | −1.003 | 0.3275 |
| 200844 | *C3orf67* | Chromosome 3 open reading frame 67 | 1.584 | −1.436 | 0.3482 |
| 57016 | *AKR1B10* | Aldo-keto reductase family 1, member B10 (aldose reductase) | 3.628 | −2.490 | 0.3591 |
| 1719 | *DHFR* | Dihydrofolate reductase | 1.538 | −1.033 | 0.4901 |
| 8581 | *LY6D* | Lymphocyte antigen 6 complex, locus D | 2.171 | −1.384 | 0.5123 |
| 6518 | *SLC2A5* | Solute carrier family 2 (facilitated glucose/fructose transporter), member 5 | 1.986 | −1.018 | 0.5410 |
| 10535 | *RNASEH2A* | Ribonuclease H2, subunit A | 1.751 | −1.020 | 0.5517 |
| 10018 | *BCL2L11* | BCL2-like 11 (apoptosis facilitator) | 1.592 | −1.310 | 0.5755 |
| 25837 | *RAB26* | RAB26, member RAS oncogene family | 2.112 | −1.420 | 0.5804 |
| 57834 | *CYP4F11* | Cytochrome P450, family 4, subfamily F, polypeptide 11 | 1.795 | −1.032 | 0.6899 |
| 100133941 | *CD24* | CD24 molecule | 2.092 | −1.777 | 0.7765 |
| 56521 | *DNAJC12* | DnaJ (Hsp40) homolog, subfamily C, member 12 | 2.208 | −1.687 | 0.7922 |
| 3141 | *HLCS* | Holocarboxylase synthetase | 1.791 | −1.020 | 0.8947 |
| 222962 | *SLC29A4* | Solute carrier family 29 (equilibrative nucleoside transporter), member 4 | 1.617 | −1.100 | 0.9072 |
| 1645 | *AKR1C1* | Aldo-keto reductase family 1, member C1 | 2.257 | −1.546 | 0.9583 |
| 152404 | *IGSF11* | Immunoglobulin superfamily, member 11 | 1.590 | −1.572 | 0.9790 |
| 85285 | *KRTAP4-1* | Keratin-associated protein 4-1 | 2.215 | −1.029 | no data |
| 25859 | *PART1* | Prostate androgen-regulated transcript 1 (non-protein coding) | 1.915 | −1.383 | no data |

## 3. Discussion

According to the current concept of miRNA biogenesis, miRNA passenger strands are degraded and have no cellular functions. In contrast to this concept, our miRNA signatures based on RNA sequencing revealed that some passenger strands are aberrantly expressed in cancer tissues [10,16,21,24–27]. Importantly, functional assays showed that some passenger strands of miRNAs (e.g., *miR-144-5p*, *miR-145-3p*, *miR-139-3p*, *miR-199-3p*, *miR-223-3p*, and *miR-455-5p*) actually acted as anti-tumor miRNAs by controlling cancer-related genes [17,25,28–33]. In general theory, passenger strand of miRNAs derived from miRNA-duplex have degraded in cytoplasm and have no function. In fact, the expression of passenger strand of miRNA is overwhelmingly lower than that of guide strand. Is the passenger strand of miRNA actually functional *in vivo*? This is an important issue in miRNA research. Expression levels of *miR-150-3p* were lower (100 ×) than *miR-150-5p* in LUAD cells. Our *in vitro* functional assays showed that antitumor effects are observed even if the transfection concentration of mature *miR-150-3p* is lowered (1 nM and 0.1 nM). Elucidation of functions of passenger strand of miRNA *in vivo* is an important biological theme. The involvement of passenger strands of miRNAs in cancer pathogenesis is an attractive proposal for cancer research. Identification of novel molecules controlled by miRNA (the passenger strand of miRNA duplex) will contribute to the understanding of the oncogenic networks of LUAD.

In previous studies, tumor suppressive function of *miR-150-5p* (the guide strand) was reported in several cancers [18,22,23]. In contrast to this, very few reports have investigated the functional significance of *miR-150-3p* (the passenger strand) in cancer cells and its controlled cancer-related genes. We have revealed anti-tumor function of *miR-150-3p* in esophageal, head and neck, and lung squamous cell carcinomas [21–23]. Moreover, we revealed *miR-150-3p* targets oncogenes involved in the focal adhesion pathways (e.g., *SPOCK1*, *TNC*, *ITGA3*, and *ITGA6*) [21–23]. Importantly, these genes were overexpressed in cancer tissues and their high expression was significantly correlated with poor prognosis [21–23].

In the present study, we finally identified four oncogenes (*TNS4*, *SFXN1*, *SKA3*, and *SPOCK1*) regulated by *miR-150-3p* in LUAD cells. Expression of these genes were significantly associated with LUAD pathogenesis. It is interesting to note that knockdown of *SPOCK1* significantly attenuated cancer cell migration and invasive abilities [21–23]. Another target gene, *SKA3*, was overexpressed in renal cell carcinoma and its aberrant expression was associated with cancer cell malignant phenotypes [32]. These data showed that target genes by *miR-150-3p* regulation closely contributed to LUAD pathogenesis and tumorigenesis. Detailed analysis of *miR-150-3p* target genes is indispensable for elucidating the molecular mechanism of LUAD.

We further investigated the oncogenic roles of *TNS4* (tensin 4) because high expression of *TNS4* was strongly associated with poor prognosis of LUAD patients (disease-free survival: $p = 0.0213$ and overall survival: $p = 0.0003$). *TNS4* (alias *CTEN*) is a member of the tensin family, which includes *TNS1*–*TNS4*. *TNS4* contains SH2 (Src homology 2) and PTB (phosphotyrosine binding) domains at the C-terminal region, both of which are shared with other tensin family members [34]. Interestingly, these domains are essential to bind integrin β1, c-Cbl, β-catenin, and Eepidermal growth factor (EGF) receptor [35,36]. Previous study showed that c-Cbl is an E3 ubiquitin protein ligase and induced EGFR ubiquitination. TNS4 bound to c-Cbl reduced EGFR ubiquitination and degradation [36]. As a result, overexpression of TNS4 stabilized EGFR and enhanced its oncogenic signaling in cancer cells [36].

Aberrant expression of *TNS4* was reported in cancers of the breast, colon, pancreas, and lung, and its expression was associated with poorer prognosis of these patients [34,37–39]. In hepatocellular carcinoma, EGF-induced extracellular signal-regulated kinase (ERK)1/2 activation enhanced TNS4 expression and these events enhanced the epithelial–mesenchymal transition (EMT) phenotype [40]. In lung cancer, TNS4 was upregulated by EGF-mediated STAT3 activation and its aberrant expression increased cancer cell invasiveness [41]. Our present data confirmed the oncogenic features of *TNS4* in LUAD cells. These finding indicate that expression of *TNS4* might be a good prognostic indicator and a promising therapeutic target for LUAD.

Finally, to investigate *TNS4*-modulated oncogenes in LUAD cells, we applied genome-wide gene expression analyses using knockdown of *TNS4*. A total of 88 genes were identified as putative *TNS4*-modulated targets in LUAD cells. Aberrant expression of nine genes (*C1QTNF6*, *TNS4*, *CDK1*, *SPAG5*, *MKI67*, *CHAF1B*, *ARHGAP11A*, *PRC1*, *RHOV*, $p < 0.001$) was closely associated with poor prognosis of patients with LUAD. Cyclin-dependent kinases (CDKs) are critical regulators of cell cycle progression and related to cancer aggressiveness. *CDK1* is essential for cycle progression during the G2/M transition and mitosis. High expression of *CDK1* is associated with poor prognosis in LUAD [42]. SPAG5 is a microtubule-associated protein and is involved in regulating cell cycle progression [43]. Overexpression of *SPAG5* was observed in NSCLC and promoted cell proliferation and invasion through activation of the Akt signaling pathway [44]. *PRC1*, which acts as an organizing anti-parallel microtubule in the central spindle in cytokinesis, is required for tumorigenesis driven by oncogenic K-RAS and loss of p53 in a mouse model for NSCLC [45]. Thus, the data revealed that many of the genes controlled by anti-tumor *miR-150-3p* and by *TNS* are closely involved in the pathogenesis of cancer. The elucidation of the novel targets controlled by anti-tumor miRNAs will accelerate comprehensive understanding of oncogenic networks of LUAD.

## 4. Materials and Methods

### *4.1. Human LUAD Specimens and Cell Lines*

In this study, 18 LUAD clinical samples and 28 normal lung samples were obtained from the patients who underwent lung surgery at Kagoshima University Hospital from 2010 to 2013. Table 1 presents the clinical characteristics of these patients. The LUAD samples were staged according to the Association for the Study of Lung Cancer TNM classification, seventh edition.

We used the two LUAD cell lines: A549 and H1299, purchased from the American Type Culture Collection (Manassas, VA, USA).

We obtained informed consent from all of the patients. The present study was approved by the Bioethics Committee of Kagoshima University (Kagoshima, Japan; approval no. 26-164).

### *4.2. RNA Extraction and Quantitative Real-Time PCR*

We carried out RNA extraction from formalin-fixed, paraffin-embedded specimens and cell lines and quantitative real-time reverse transcription-PCR (qRT-PCR) as previously described [18,46–48]. The TaqMan probes and primers were listed in Table S1.

### *4.3. Transfection of miRNAs, siRNAs, and Plasmid Vectors into LUAD Cells*

Transfection protocol of miRNA or siRNA species into cancer cells was described in our previous studies [18,46–48]. The reagents used in this study are listed in Table S1.

### *4.4. Incorporation of miR-150-5p or miR-150-3p into the RISC by Ago2 Immunoprecipitation*

A549 cells were transfected with 10 nM miRNAs by reverse transfection. After 72 h, immunoprecipitation was performed using a microRNA Isolation Kit, Human Ago2 (Wako Pure Chemical Industries, Ltd., Osaka, Japan) as described previously [47,48]. Expression levels of *miR-150-5p* and *miR-150-3p* were analyzed by qRT-PCR. MiRNA data were normalized to expressions of *miR-16-5p*, *miR-21-5p*, and *miR-26a*, which were not affected by *miR-150-5p* and *miR-150-3p*.

### *4.5. Cell Proliferation, Migration, and Invasion Assays*

The procedures for assessing cell proliferation, migration and invasion were described previously [18,46–48].

### *4.6. Identification of Putative Target Genes Regulated by miR-150-5p and miR-150-3p in LUAD Cells*

We identified putative target genes possessing sequences binding to *miR-150-5p* and *miR-150-3p* from the TargetScanHuman database (http://www.targetscan.org/vert_72/). GEO databases GSE19188 and GSE93290 was used for assessment of the association between target genes and the expression of NSCLC clinical specimens. Our strategy for identification of *miR-150-5p* and *miR-150-3p* target genes is outlined in Figure S3A,B.

### *4.7. Plasmid Construction and Dual Luciferase Reporter Assay*

The following two sequences were cloned into the psiCHECK-2 vector (C8021; Promega, Madison, WI, USA): the wild-type sequence of the 3′ untranslated regions (UTRs) of *TNS4*, or the deletion type, which lacked the *miR-150-3p* target sites from *TNS4*. The procedures for transfection and dual luciferase reporter assays were provided in previous studies [47,48].

### *4.8. Clinical Database Analysis of LUAD*

We investigated the clinical significance of miRNAs and their target genes with TCGA (https://tcga-data.nci.nih.gov/tcga/) in LUAD. Gene expression and clinical data were obtained from cBioPortal (http://www.cbioportal.org/) and OncoLnc (http://www.oncolnc.org/) (data downloaded on 28 September 2018) [46–49].

### *4.9. Western Blotting and Immunohistochemistry*

The procedures for Western blotting and immunohistochemistry were described previously [18,46–48]. A tissue microarray was bought from US Biomax (catalog no: BC04002a; Derwood, MD, USA). Primary antibodies were shown in Table S1.

### *4.10. Statistical Analysis*

To assess the significance of differences between two groups, we used Mann–Whitney *U* tests. Differences between multiple groups were assessed by one-way ANOVA and Tukey tests for post-hoc analysis. Tests utilized GraphPad Prism7 (GraphPad Software, La Jolla, CA, USA) and JMP Pro 14 (SAS Institute Inc., Cary, NC, USA).

## 5. Conclusions

Our results showed that the expression of both strands of the pre-*miR-150* duplex was significantly downregulated in LUAD clinical specimens and the *miR-150* duplex acted as an anti-tumor miRNA in LUAD cells. Involvement of the passenger strand of miRNA in LUAD oncogenesis suggests new possible mechanisms of pathogenesis. A total of 26 genes regulated by *miR-150-3p* were closely associated with LUAD pathogenesis. Among these targets, aberrant expression of *TNS4* enhanced cancer aggressiveness, suggesting that *TNS4* could be a promising therapeutic target for LUAD.

**Supplementary Materials:** The following are available online at http://www.mdpi.com/2072-6694/11/5/601/s1. Figure S1: Functional assays of *miR-150-3p* (0.1 nM, 1 nM, 10 nM) in LUAD cells (A549 and H1299), Figure S2: Both strands of *miR-150-5p* and *miR-150-3p* were incorporated into the RISC, Figure S3: The strategy for identification of genes regulated by *miR-150-5p* and *miR-150-3p*, Figure S4: *TNS4* was directly suppressed at the diluted concentration of *miR-150-3p* precursor (1 nM and 0.1 nM), Figure S5: The nucleotide sequences of 3′UTR of *TNS4* in A549 cells, Figure S6: The strategy for identification of *TNS4*-modulated genes, Table S1: Reagent used in this study, Table S2: Immunohistochemical status and characteristics of the lung cancer and non-cancerous cases.

**Author Contributions:** Conceptualization, S.M., N.S. and H.I.; methodology, N.S.; validation, A.U., H.S. and T.K.; formal analysis, S.M. and T.K.; investigation, N.S., S.M. and K.M.; resources, N.S., K.M., Y.Y., N.K., T.S. and H.I.; writing—original draft preparation, S.M. and N.S.; writing—review and editing, N.S., K.M., Y.Y., A.U., H.S., T.K. and T.S.; visualization, S.M. and T.K.; supervision, N.S.; funding acquisition, N.S., N.K., T.K. and H.I.

**Funding:** This research was funded by KAKENHI grants, 17K09660 and 18K09338.

**Conflicts of Interest:** The authors declare no conflict of interest.

## References


1. Ferlay, J.; Colombet, M.; Soerjomataram, I.; Mathers, C.; Parkin, D.M.; Pineros, M.; Znaor, A.; Bray, F. Estimating the global cancer incidence and mortality in 2018: GLOBOCAN sources and methods. *Int. J. Cancer* **2018**. [CrossRef]
2. Cheng, T.Y.; Cramb, S.M.; Baade, P.D.; Youlden, D.R.; Nwogu, C.; Reid, M.E. The International Epidemiology of Lung Cancer: Latest Trends, Disparities, and Tumor Characteristics. *J. Thorac. Oncol. Off. Publ. Int. Assoc. Study Lung Cancer* **2016**, *11*, 1653–1671. [CrossRef] [PubMed]
3. Herbst, R.S.; Morgensztern, D.; Boshoff, C. The biology and management of non-small cell lung cancer. *Nature* **2018**, *553*, 446–454. [CrossRef] [PubMed]
4. Heyneman, L.E.; Herndon, J.E.; Goodman, P.C.; Patz, E.F., Jr. Stage distribution in patients with a small (< or = 3 cm) primary nonsmall cell lung carcinoma. Implication for lung carcinoma screening. *Cancer* **2001**, *92*, 3051–3055. [PubMed]
5. Lin, P.Y.; Chang, Y.C.; Chen, H.Y.; Chen, C.H.; Tsui, H.C.; Yang, P.C. Tumor size matters differently in pulmonary adenocarcinoma and squamous cell carcinoma. *Lung Cancer* **2010**, *67*, 296–300. [CrossRef]
6. Goldstraw, P.; Chansky, K.; Crowley, J.; Rami-Porta, R.; Asamura, H.; Eberhardt, W.E.; Nicholson, A.G.; Groome, P.; Mitchell, A.; Bolejack, V. The IASLC Lung Cancer Staging Project: Proposals for Revision of the TNM Stage Groupings in the Forthcoming (Eighth) Edition of the TNM Classification for Lung Cancer. *J. Thorac. Oncol. Off. Publ. Int. Assoc. Study Lung Cancer* **2016**, *11*, 39–51. [CrossRef]
7. Bartel, D.P. MicroRNAs: Target recognition and regulatory functions. *Cell* **2009**, *136*, 215–233. [CrossRef]
8. Goto, Y.; Kurozumi, A.; Enokida, H.; Ichikawa, T.; Seki, N. Functional significance of aberrantly expressed microRNAs in prostate cancer. *Int. J. Urol. Off. J. Jpn. Urol. Assoc.* **2015**, *22*, 242–252. [CrossRef]
9. Catalanotto, C.; Cogoni, C.; Zardo, G. MicroRNA in Control of Gene Expression: An Overview of Nuclear Functions. *Int. J. Mol. Sci.* **2016**, *17*, 1712. [CrossRef]
10. Koshizuka, K.; Hanazawa, T.; Fukumoto, I.; Kikkawa, N.; Okamoto, Y.; Seki, N. The microRNA signatures: Aberrantly expressed microRNAs in head and neck squamous cell carcinoma. *J. Hum. Genet.* **2017**, *62*, 3–13. [CrossRef]
11. Mizuno, K.; Mataki, H.; Seki, N.; Kumamoto, T.; Kamikawaji, K.; Inoue, H. MicroRNAs in non-small cell lung cancer and idiopathic pulmonary fibrosis. *J. Hum. Genet.* **2017**, *62*, 57–65. [CrossRef]
12. Gulyaeva, L.F.; Kushlinskiy, N.E. Regulatory mechanisms of microRNA expression. *J. Transl. Med.* **2016**, *14*, 143. [CrossRef]
13. Ramassone, A.; Pagotto, S.; Veronese, A.; Visone, R. Epigenetics and MicroRNAs in Cancer. *Int. J. Mol. Sci.* **2018**, *19*, 459. [CrossRef] [PubMed]
14. Kumamoto, T.; Seki, N.; Mataki, H.; Mizuno, K.; Kamikawaji, K.; Samukawa, T.; Koshizuka, K.; Goto, Y.; Inoue, H. Regulation of TPD52 by antitumor microRNA-218 suppresses cancer cell migration and invasion in lung squamous cell carcinoma. *Int. J. Oncol.* **2016**, *49*, 1870–1880. [CrossRef] [PubMed]
15. Mataki, H.; Seki, N.; Mizuno, K.; Nohata, N.; Kamikawaji, K.; Kumamoto, T.; Koshizuka, K.; Goto, Y.; Inoue, H. Dual-strand tumor-suppressor microRNA-145 (miR-145-5p and miR-145-3p) coordinately targeted MTDH in lung squamous cell carcinoma. *Oncotarget* **2016**, *7*, 72084–72098. [CrossRef]
16. Mizuno, K.; Mataki, H.; Arai, T.; Okato, A.; Kamikawaji, K.; Kumamoto, T.; Hiraki, T.; Hatanaka, K.; Inoue, H.; Seki, N. The microRNA expression signature of small cell lung cancer: Tumor suppressors of miR-27a-5p and miR-34b-3p and their targeted oncogenes. *J. Hum. Genet.* **2017**, *62*, 671–678. [CrossRef]
17. Misono, S.; Seki, N.; Mizuno, K.; Yamada, Y.; Uchida, A.; Arai, T.; Kumamoto, T.; Sanada, H.; Suetsugu, T.; Inoue, H. Dual strands of the miR-145 duplex (miR-145-5p and miR-145-3p) regulate oncogenes in lung adenocarcinoma pathogenesis. *J. Hum. Genet.* **2018**, *63*, 1015–1028. [CrossRef]
18. Suetsugu, T.; Koshizuka, K.; Seki, N.; Mizuno, K.; Okato, A.; Arai, T.; Misono, S.; Uchida, A.; Kumamoto, T.; Inoue, H. Downregulation of matrix metalloproteinase 14 by the antitumor miRNA, miR-150-5p, inhibits the aggressiveness of lung squamous cell carcinoma cells. *Int. J. Oncol.* **2018**, *52*, 913–924. [CrossRef] [PubMed]
19. Uchida, A.; Seki, N.; Mizuno, K.; Misono, S.; Yamada, Y.; Kikkawa, N.; Sanada, H.; Kumamoto, T.; Suetsugu, T.; Inoue, H. Involvement of dual-strand of the miR-144 duplex and their targets in the pathogenesis of lung squamous cell carcinoma. *Cancer Sci.* **2018**. [CrossRef] [PubMed]
20. Matranga, C.; Tomari, Y.; Shin, C.; Bartel, D.P.; Zamore, P.D. Passenger-strand cleavage facilitates assembly of siRNA into Ago2-containing RNAi enzyme complexes. *Cell* **2005**, *123*, 607–620. [CrossRef] [PubMed]

21. Koshizuka, K.; Nohata, N.; Hanazawa, T.; Kikkawa, N.; Arai, T.; Okato, A.; Fukumoto, I.; Katada, K.; Okamoto, Y.; Seki, N. Deep sequencing-based microRNA expression signatures in head and neck squamous cell carcinoma: Dual strands of pre-miR-150 as antitumor miRNAs. *Oncotarget* **2017**, *8*, 30288–30304. [CrossRef]
22. Osako, Y.; Seki, N.; Koshizuka, K.; Okato, A.; Idichi, T.; Arai, T.; Omoto, I.; Sasaki, K.; Uchikado, Y.; Kita, Y.; et al. Regulation of SPOCK1 by dual strands of pre-miR-150 inhibit cancer cell migration and invasion in esophageal squamous cell carcinoma. *J. Hum. Genet.* **2017**, *62*, 935–944. [CrossRef] [PubMed]
23. Koshizuka, K.; Hanazawa, T.; Kikkawa, N.; Katada, K.; Okato, A.; Arai, T.; Idichi, T.; Osako, Y.; Okamoto, Y.; Seki, N. Antitumor miR-150-5p and miR-150-3p inhibit cancer cell aggressiveness by targeting SPOCK1 in head and neck squamous cell carcinoma. *AurisNasusLarynx* **2018**, *45*, 854–865. [CrossRef]
24. Goto, Y.; Kurozumi, A.; Nohata, N.; Kojima, S.; Matsushita, R.; Yoshino, H.; Yamazaki, K.; Ishida, Y.; Ichikawa, T.; Naya, Y.; et al. The microRNA signature of patients with sunitinib failure: Regulation of UHRF1 pathways by microRNA-101 in renal cell carcinoma. *Oncotarget* **2016**, *7*, 59070–59086. [CrossRef]
25. Goto, Y.; Kurozumi, A.; Arai, T.; Nohata, N.; Kojima, S.; Okato, A.; Kato, M.; Yamazaki, K.; Ishida, Y.; Naya, Y.; et al. Impact of novel miR-145-3p regulatory networks on survival in patients with castration-resistant prostate cancer. *Br. J. Cancer* **2017**, *117*, 409–420. [CrossRef]
26. Yonemori, K.; Seki, N.; Idichi, T.; Kurahara, H.; Osako, Y.; Koshizuka, K.; Arai, T.; Okato, A.; Kita, Y.; Arigami, T.; et al. The microRNA expression signature of pancreatic ductal adenocarcinoma by RNA sequencing: Anti-tumour functions of the microRNA-216 cluster. *Oncotarget* **2017**, *8*, 70097–70115. [CrossRef]
27. Toda, H.; Kurozumi, S.; Kijima, Y.; Idichi, T.; Shinden, Y.; Yamada, Y.; Arai, T.; Maemura, K.; Fujii, T.; Horiguchi, J.; et al. Molecular pathogenesis of triple-negative breast cancer based on microRNA expression signatures: Antitumor miR-204-5p targets AP1S3. *J. Hum. Genet.* **2018**, *63*, 1197–1210. [CrossRef] [PubMed]
28. Yonemori, M.; Seki, N.; Yoshino, H.; Matsushita, R.; Miyamoto, K.; Nakagawa, M.; Enokida, H. Dual tumor-suppressors miR-139-5p and miR-139-3p targeting matrix metalloprotease 11 in bladder cancer. *Cancer Sci.* **2016**, *107*, 1233–1242. [CrossRef] [PubMed]
29. Koshizuka, K.; Hanazawa, T.; Kikkawa, N.; Arai, T.; Okato, A.; Kurozumi, A.; Kato, M.; Katada, K.; Okamoto, Y.; Seki, N. Regulation of ITGA3 by the anti-tumor miR-199 family inhibits cancer cell migration and invasion in head and neck cancer. *Cancer Sci.* **2017**, *108*, 1681–1692. [CrossRef] [PubMed]
30. Sugawara, S.; Yamada, Y.; Arai, T.; Okato, A.; Idichi, T.; Kato, M.; Koshizuka, K.; Ichikawa, T.; Seki, N. Dual strands of the miR-223 duplex (miR-223-5p and miR-223-3p) inhibit cancer cell aggressiveness: Targeted genes are involved in bladder cancer pathogenesis. *J. Hum. Genet.* **2018**, *63*, 657–668. [CrossRef] [PubMed]
31. Yamada, Y.; Arai, T.; Kojima, S.; Sugawara, S.; Kato, M.; Okato, A.; Yamazaki, K.; Naya, Y.; Ichikawa, T.; Seki, N. Regulation of antitumor miR-144-5p targets oncogenes: Direct regulation of syndecan-3 and its clinical significance. *Cancer Sci.* **2018**, *109*, 2919–2936. [CrossRef] [PubMed]
32. Yamada, Y.; Arai, T.; Kojima, S.; Sugawara, S.; Kato, M.; Okato, A.; Yamazaki, K.; Naya, Y.; Ichikawa, T.; Seki, N. Anti-tumor roles of both strands of the miR-455 duplex: Their targets SKA1 and SKA3 are involved in the pathogenesis of renal cell carcinoma. *Oncotarget* **2018**, *9*, 26638–26658. [CrossRef]
33. Yamada, Y.; Koshizuka, K.; Hanazawa, T.; Kikkawa, N.; Okato, A.; Idichi, T.; Arai, T.; Sugawara, S.; Katada, K.; Okamoto, Y.; et al. Passenger strand of miR-145-3p acts as a tumor-suppressor by targeting MYO1B in head and neck squamous cell carcinoma. *Int. J. Oncol.* **2018**, *52*, 166–178. [CrossRef]
34. Lo, S.H. C-terminal tensin-like (CTEN): A promising biomarker and target for cancer. *Int. J. Biochem. Cell Biol.* **2014**, *51*, 150–154. [CrossRef]
35. Katz, M.; Amit, I.; Citri, A.; Shay, T.; Carvalho, S.; Lavi, S.; Milanezi, F.; Lyass, L.; Amariglio, N.; Jacob-Hirsch, J.; et al. A reciprocal tensin-3-cten switch mediates EGF-driven mammary cell migration. *Nat. Cell Biol.* **2007**, *9*, 961–969. [CrossRef]
36. Hong, S.Y.; Shih, Y.P.; Li, T.; Carraway, K.L., 3rd; Lo, S.H. CTEN prolongs signaling by EGFR through reducing its ligand-induced degradation. *Cancer Res.* **2013**, *73*, 5266–5276. [CrossRef]
37. Liao, Y.C.; Chen, N.T.; Shih, Y.P.; Dong, Y.; Lo, S.H. Up-regulation of C-terminal tensin-like molecule promotes the tumorigenicity of colon cancer through beta-catenin. *Cancer Res.* **2009**, *69*, 4563–4566. [CrossRef] [PubMed]
38. Albasri, A.; Al-Ghamdi, S.; Fadhil, W.; Aleskandarany, M.; Liao, Y.C.; Jackson, D.; Lobo, D.N.; Lo, S.H.; Kumari, R.; Durrant, L.; et al. Cten signals through integrin-linked kinase (ILK) and may promote metastasis in colorectal cancer. *Oncogene* **2011**, *30*, 2997–3002. [CrossRef] [PubMed]

39. Al-Ghamdi, S.; Cachat, J.; Albasri, A.; Ahmed, M.; Jackson, D.; Zaitoun, A.; Guppy, N.; Otto, W.R.; Alison, M.R.; Kindle, K.B.; et al. C-terminal tensin-like gene functions as an oncogene and promotes cell motility in pancreatic cancer. *Pancreas* **2013**, *42*, 135–140. [CrossRef] [PubMed]
40. Chan, L.K.; Chiu, Y.T.; Sze, K.M.; Ng, I.O. Tensin4 is up-regulated by EGF-induced ERK1/2 activity and promotes cell proliferation and migration in hepatocellular carcinoma. *Oncotarget* **2015**, *6*, 20964–20976. [CrossRef]
41. Bennett, D.T.; Reece, T.B.; Foley, L.S.; Sjoberg, A.; Meng, X.; Fullerton, D.A.; Weyant, M.J. C-terminal tensin-like protein mediates invasion of human lung cancer cells and is regulated by signal transducer and activator of transcription 3. *J. Thorac. Cardiovasc. Surg.* **2015**, *149*, 369–375. [CrossRef]
42. Shi, Y.X.; Zhu, T.; Zou, T.; Zhuo, W.; Chen, Y.X.; Huang, M.S.; Zheng, W.; Wang, C.J.; Li, X.; Mao, X.Y.; et al. Prognostic and predictive values of CDK1 and MAD2L1 in lung adenocarcinoma. *Oncotarget* **2016**, *7*, 85235–85243. [CrossRef]
43. Gruber, J.; Harborth, J.; Schnabel, J.; Weber, K.; Hatzfeld, M. The mitotic-spindle-associated protein astrin is essential for progression through mitosis. *J. Cell Sci.* **2002**, *115*, 4053–4059. [CrossRef]
44. Song, L.; Dai, Z.; Zhang, S.; Zhang, H.; Liu, C.; Ma, X.; Liu, D.; Zan, Y.; Yin, X. MicroRNA-1179 suppresses cell growth and invasion by targeting sperm-associated antigen 5-mediated Akt signaling in human non-small cell lung cancer. *Biochem. Biophys. Res. Commun.* **2018**, *504*, 164–170. [CrossRef]
45. Hanselmann, S.; Wolter, P.; Malkmus, J.; Gaubatz, S. The microtubule-associated protein PRC1 is a potential therapeutic target for lung cancer. *Oncotarget* **2018**, *9*, 4985–4997. [CrossRef]
46. Kamikawaji, K.; Seki, N.; Watanabe, M.; Mataki, H.; Kumamoto, T.; Takagi, K.; Mizuno, K.; Inoue, H. Regulation of LOXL2 and SERPINH1 by antitumor microRNA-29a in lung cancer with idiopathic pulmonary fibrosis. *J. Hum. Genet.* **2016**, *61*, 985–993. [CrossRef]
47. Arai, T.; Kojima, S.; Yamada, Y.; Sugawara, S.; Kato, M.; Yamazaki, K.; Naya, Y.; Ichikawa, T.; Seki, N. Pirin: A potential novel therapeutic target for castration-resistant prostate cancer regulated by miR-455-5p. *Mol. Oncol.* **2018**. [CrossRef]
48. Yamada, Y.; Sugawara, S.; Arai, T.; Kojima, S.; Kato, M.; Okato, A.; Yamazaki, K.; Naya, Y.; Ichikawa, T.; Seki, N. Molecular pathogenesis of renal cell carcinoma: Impact of the anti-tumor miR-29 family on gene regulation. *Int. J. Urol. Off. J. Jpn. Urol. Assoc.* **2018**, *25*, 953–965. [CrossRef]
49. Gao, J.; Aksoy, B.A.; Dogrusoz, U.; Dresdner, G.; Gross, B.; Sumer, S.O.; Sun, Y.; Jacobsen, A.; Sinha, R.; Larsson, E.; et al. Integrative analysis of complex cancer genomics and clinical profiles using the cBioPortal. *Sci. Signal.* **2013**, *6*, pl1. [CrossRef]


# Supplementary Materials: Molecular pathogenesis of gene regulation by the *miR-150* duplex: *miR-150-3p* regulates *TNS4* in lung adenocarcinoma

**Shunsuke Misono, Naohiko Seki, Keiko Mizuno, Yasutaka Yamada, Akifumi Uchida, Hiroki Sanada, Shogo Moriya, Naoko Kikkawa, Tomohiro Kumamoto, Takayuki Suetsugu and Hiromasa Inoue**

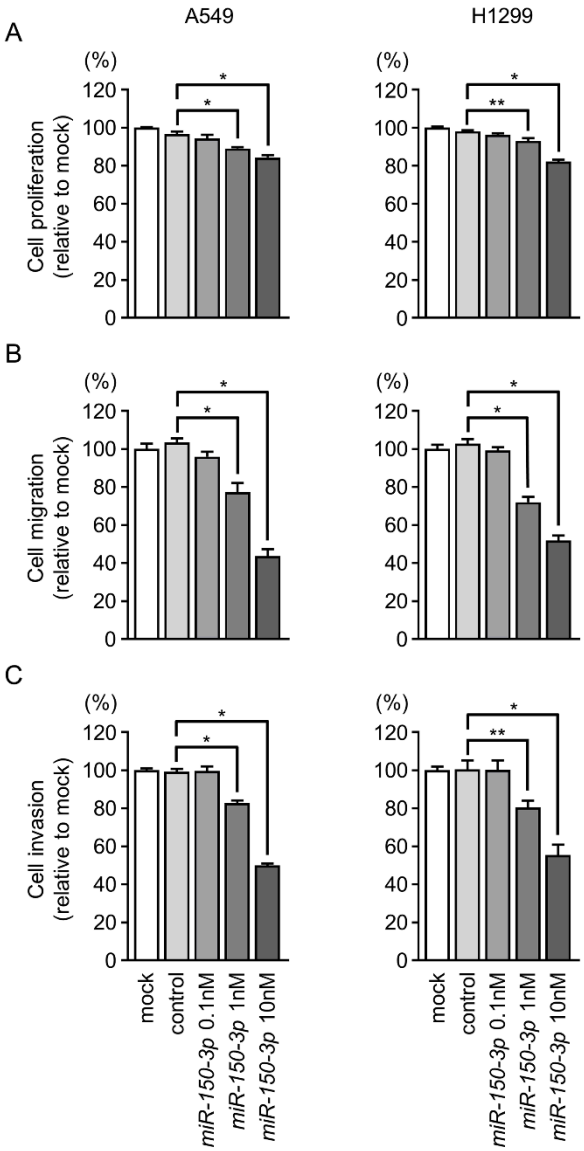


**Figure S1.** Functional assays of *miR-150-3p* (0.1 nM, 1 nM, 10 nM) in LUAD cells (A549 and H1299). (A-C) Cell proliferation, migration, and invasive activities were significantly blocked by ectopic expression of *miR-150-3p* with 1 nM and 10 nM concentration. * $p < 0.01$, ** $p < 0.05$.

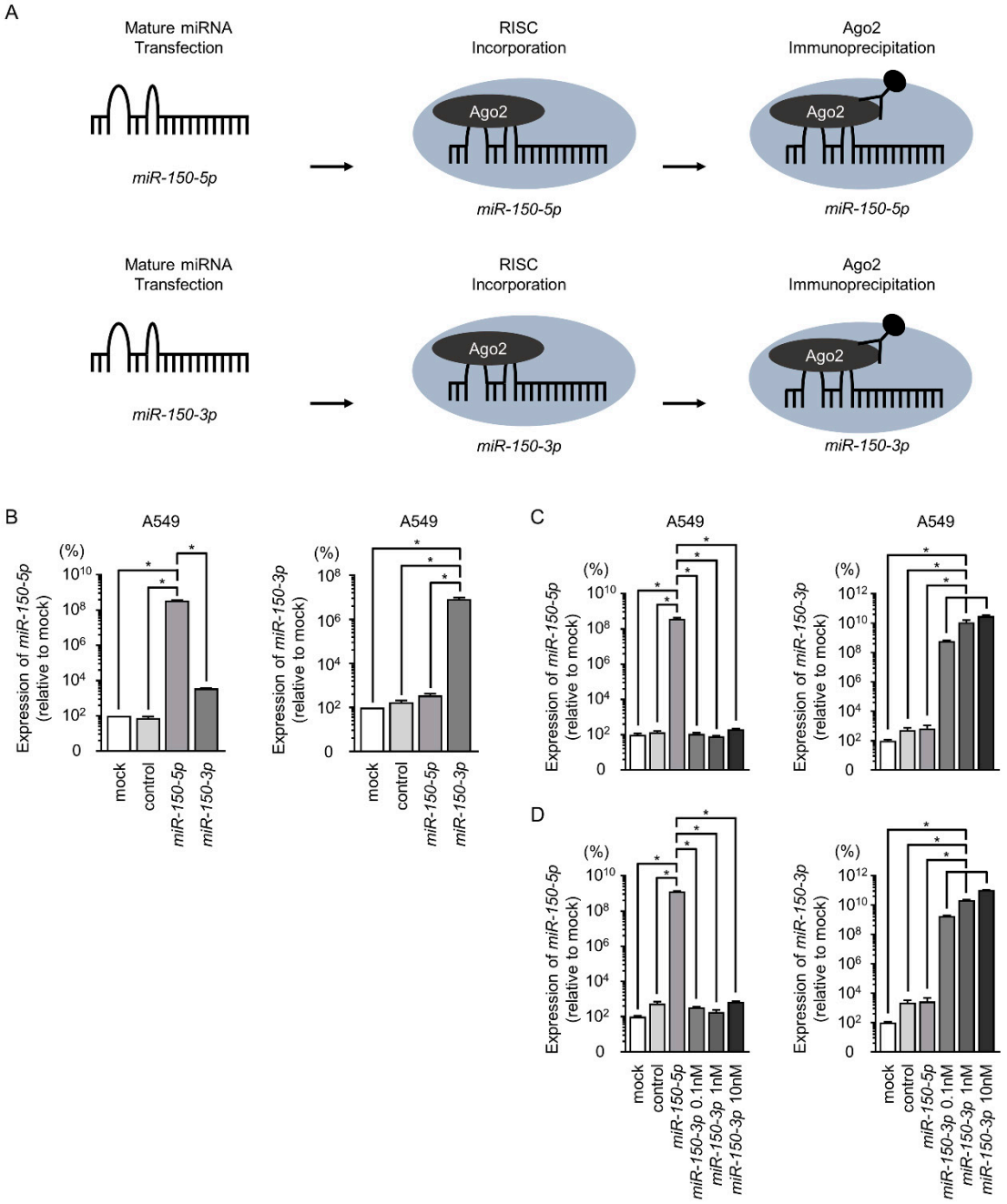


**Figure S2.** Both strands of *miR-150-5p* and *miR-150-3p* were incorporated into the RISC. (**A**) Schematic diagram for isolation of the Ago2-miRNA complex from the RISC. (**B–D**) Expression levels of *miR-150-5p* or *miR-150-3p* bound to Ago2 were measured by TaqMan RT-qPCR and normalized to the expression of *miR-26a* (**B**), *miR-16-5p* (**C**) and *miR-21-5p* (**D**), which had no effect upon *miR-150-5p* and *miR-150-3p*. * $p < 0.01$.

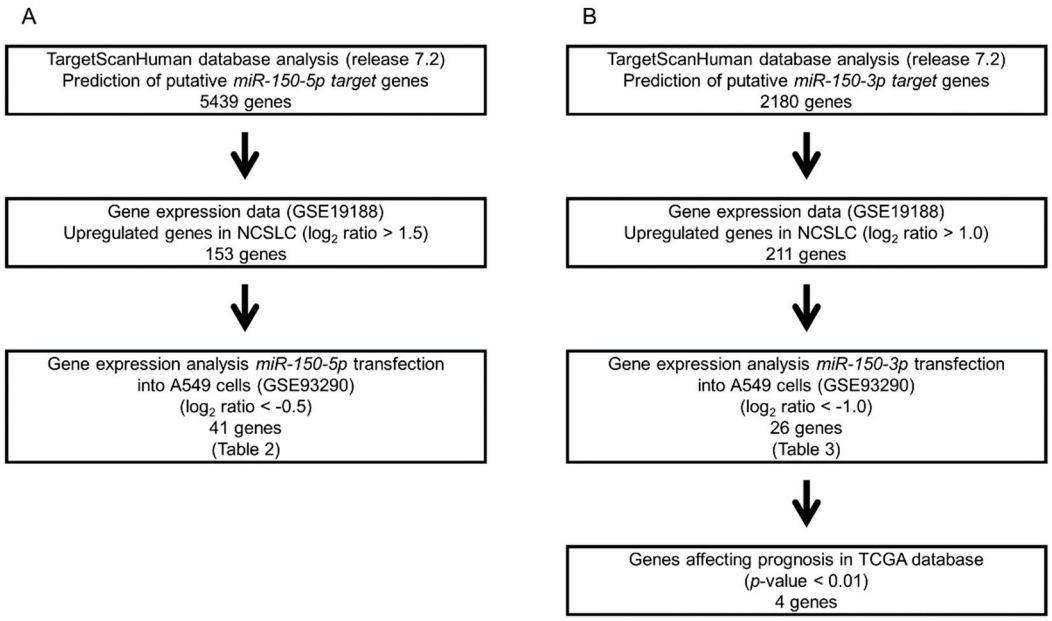


**Figure S3.** The strategy for identification of genes regulated by *miR-150-5p* and *miR-150-3p*. We obtained putative genes regulated by *miR-150-5p* and *miR-150-3p* using the TargetScanHuman Release 7.2 database and selected upregulated genes in non-small cell lung cancer clinical expression profiles from the GEO database (GSE19188). Then, we combined the gene expression analyses using A549 cells transfected with *miR-150-5p* or *miR-150-3p* and inspected the downregulated genes (GSE93290).

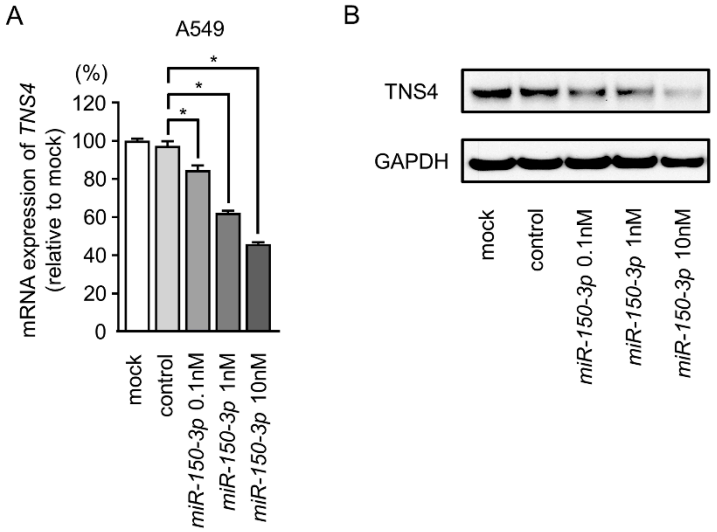


**Figure S4.** *TNS4* was directly suppressed at the diluted concentration of *miR-150-3p* precursor (1 nM and 0.1 nM). (**A**,**B**) *TNS4* mRNA and protein expression was reduced by *miR-150-3p* ectopic expression (48h after transfection). *GUSB* was used as an expression control. GAPDH was used as a loading control. * $p < 0.01$.

*TNS4* 3'UTR variant 1

GACAGAGCCTCAGGAGAACGTATGCCACCTCTTTGCGGAGTATGACATGGTCCAGCCAGC
CTCGCAGGTCATCGGCCTGGTGACTGCTCTGCTGCAGGACGCAGAAAGGATGTAGGGGAG
AAACTGCCTGTGCACCTAACCAACACCTCCAGGGGCCCGCTAAGGAGCCCCCCTCCACCC

CCTGAATGGGTGTGGCTTGTGGCCATATTGACAGACCAATCTATGGGACTAGGGGGATTG
GCATCAAGTTGAAACCCCATCTCTACAAAGAATACAAAAATTAGCCGGGCAAGGTAGCGC
ACCTGTGGTCCCAGGTACTCGGGAGACTGAGGCATGAGAATCCCTTGAAACTGGGAGGCG
GAAGTTGCAGTGAGCTGTGATCGTGCCACTGCACTCCAGCCTGGTTGACAGAGCAACATG
CTATCTCTAAAACAAACAAACAAACAAAAACTCAGGTTCCCACACCCTCTAAACCCTGCC
TCCTCTCAGGCTACAGAGACCTCTCCAGGAGGCTGAAGTGCCCTTACCCCGACCATCTGA
CCAGCCACCGCCCCATGCCCGTGCCCCACCGAGGGCGGAGGCTGCTCACTGCTCTGTTTT
ATCTCTGGCCTCTGATCCTGCATTCTTGTGCCAGGGCTTAGACCCAGGGCAAGGTCTTAG
ACCCAGGGCAGGGGTAGGGTTAAAGGCTTTCAACCCAGGGGCCAGTGCCTTAATTCATGC
AACAAATGTTTTCTGGCTGTGTGCTTTATTCATGTGAACCAGGAAAACAGAAAAATATGA
CAGTGTTTCCAACAGAGGTTTATAAGTGCTATGCAGGGCTGGTGGAAAGAGTAGAAACTG
AGAAAGATAAACTTTACCCACTTGAAGGGAAGGAGGGCAATGTTACCAAGAAGGTAACAT
TTGAGTTGGGTCTTCAAGGATGAATAGGAGTTCGGCATGCAAAGAGAGTTAGAAACCAAC
TTTTAGGAGTGGGGAGGGGCTCTCATGTGCTACATACAATCTGAGGCACATTATATATGC
CTAATCCCATTTTACAGATTAGAAAACTGGGGCTCAGAGGGTTAACTTGCCCACATTCAC
CTAACTGTAAATGGCAGAGAAACAGGATTTCAAGTCCATGCCCATCCTATTGCCCCAGCA
TTCACAGAAAGCAGATGGAGACATTCGTGTGTGAAGCACACAGGTATGAAAAGATGTACC
AAGTTTGGTGTGGCTCAAGTACATGGTACCTAAGGGAGTAGGTGAGAGAGAAAGCAGAAG

*TNS4* 3'UTR variant 2

GACAGAGCCTCAGGAGAACGTATGCCACCTCTTTGCGGAGTATGACATGGTCCAGCCAGC
CTCGCAGGTCATCGGCCTGGTGACTGCTCTGCTGCAGGACGCAGAAAGGATGTAGGGGAG
AGACTGCCTGTGCACCTAACCAACACCTCCAGGGGCTCGCTAAGGAGCCCCCCTCCACCC
CCTGAATGGGTGTGGCTTGTGGCCATATTGACAGACCAATCTATGGGACTAGGGGGATTG
GCATCAAGTTGACACCCTTGAACCTGCTATGGCCTTCAGCAGTCACCATCATCCAGACCC
CCCGGGCCTCAGTTTCCTCAATCATAGAAGAAGACCAATAGACAAGATCAGCTGTTCTTA
GATGCTGGTGGGCATTTGAACATGCTCCTCCATGATTCTGAAGCATGCACACCTCTGAAG
ACCCCTGCATGAAAATAACCTCCAAGGACCCTCTGACCCCATCGACCTGGGCCCTGCCCA
CACAACAGTCTGAGCAAGAGACCTGCAGCCCCTGTTTCGTGGCAGACAGCAGGTGCCTGG
CGGTGACCCACGGGGCTCCTGGCTTGCAGCTGGTGATGGTCAAGAACTGACTACAAAACA
GGAATGGATAGACTCTATTTCCTTCCATATCTGTTCCTCTGTTCCTTTTCCCACTTTCTG
GGTGGCTTTTTGGGTCCACCCAGCCAGGATGCTGCAGGCCAAGCTGGGTGTGGTATTTAG
GGCAGCTCAGCAGGGGGAACTTGTCCCCATGGTCAGAGGAGACCCAGCTGTCCTGCACCC
CCTTGCAGATGAGTATCACCCCATCTTTTCTTTCCACTTGTTTTTTATTTTTATTTTTTT
TGAGACAGAGTCTCACTGTCACCCAGGCTGAACTGCAGTGGTGTGATCTAGGCTCACTGC
AACCTCCACCTCCCAGGTACTCAGGAGACTGAGGCATGAGAATCCCTTGAAACTGGGAGG
CGGAAGTTGCAGTGAGCTGTGATCGTGCCACTGCACTCCAGCCTGGTTGACAGAGCAACA
TGCTATCTCTAAAACAAACAAACAAACAAAAACTCAGGTTCCCACACCCTCTAAACCCTG
CCTCCTCTCAGGCTACAGAGACCTCTCCAGGAGGCTGAAGTGCCCTTACCCCGACCATCT
GACCAGCCACCGCCCCATGCCCGTGCCCCACCGAGGGCGGAGGCTGCTCACTGCTCTGTT
TTATCTCTGGCCTCTGATCCTGCATTCTTGTGCCAGGGCTTAGACCCAGGGCAAGGTCTT
AGACCCAGGGCAGGGGTAGGGTTAAAGGCTTTCAACCCAGGGGCCAGTGCCTTAATTCAT
GCAACAAATGTTTTCTGGCTGTGTGCTTTATTCATGTGAACCAGGAAAACAGAAAAATAT

GACAGTGTTTCCAACAGAGGTTTATAAGTGCTATGCAGGGCTGGTGGAAAGAGTAGAAAC
TGAGAAAGATAAACTTTACCCACTTGAAGGGAAGGAGGGCAATGTTACCAAGAAGGTAAC
ATTTGAGTTGGGTCTTCAAGGATGAATAGGAGTTCGGCATGCAAAGAGAGTTAGAAACCA
ACTTTTAGGAGTGGGGAGGGGCTCTCATGTGCTACATACAATCTGAGGCACATTATATAT
GCCTAATCCCATTTTACAGATTAGAAAACTGGGGCTCAGAGGGTTAACTTGCCCACATTC
ACCTAACTGTAAATGGCAGAGAAACAGGATTTCAAGTCCATGCCCATCCTATTGCCCCAG
CATTCACAGAAAGCAGATGGAGACATTCGTGTGTGAAGCACACAGGTATGAAAAGATGTA
CCAAGTTTGGTGTGGCTCAAGTACATGGTACCTAAGGGAGTAGGTGAGAGAGAAAGCAGA

*TNS4* 3'UTR variant 3

GACAGAGCCTCAGGAGAACGTATGCCACCTCTTTGCGGAGTATGACATGGTCCAGCCAGC
CTCGCAGGTCATCGGCCTGGTGACTGCTCTGCTGCAGGACGCAGAAAGGATGTAGGGGAG
AGACTGCCTGTGCACCTAACCAACACCTCCAGGGGCTCGCTAAGGAGCCCCCCTCCACCC
CCTGAATGGGTGTGGCTTGTGGCCATATTGACAGACCAATCTATGGGACTAGGGGGATTG
GCATCAAGTTGACACCCTTGAACCTGCTATGGCCTTCAGCAGTCACCATCATCCAGACCC
CCCGGGCCTCAGTTTCCTCAATCATAGAAGAAGACCAATAGACAAGATCAGCTGTTCTTA
GATGCTGGTGGGCATTTGAACATGCTCCTCCATGATTCTGAAGCATGCACACCTCTGAAG
ACCCCTGCATGAAAATAACCTCCAAGGACCCTCTGACCCCATCGACCTGGGCCCTGCCCA
CACAACAGTCTGAGCAAGAGACCTGCAGCCCCTGTTTCGTGGCAGACAGCAGGTGCCTGG
CGGTGACCCACGGGGCTCCTGGCTTGCAGCTGGTGATGGTCAAGAACTGACTACAAAACA
GGAATGGATAGACTCTATTTCCTTCCATATCTGTTCCTCTGTTCCTTTTCCCACTTTCTG
GGTGGCTTTTTGGGTCCACCCAGCCAGGATGCTGCAGGCCAAGCTGGGTGTGGTATTTAG
GGCAGCTCAGCAGGGGGAACTTGTCCCCATGGTCAGAGGAGACCCAGCTGTCCTGCACCC
CCTTGCAGATGAGTATCACCCCATCTTTTCTTTCCACTTGTTTTTTATTTTTATTTTTTT
TGAGACAGAGTCTCACTGTCACCCAGGCTGAACTGCAGTGGTGTGATCTAGGCTCACTGC
AACCTCCACCTCCCAGGTTCAAGCAATTATCCTGCCTCAGGCTCCCAAGTAGCTGGGATT
ACAGGCATGTGCAACTCACCCAGCTAATTTTGTATTTTTAGTAGAAACATGGTGAAACCC
CATCTCTACAAAAAATACAAAAATTAGCCGGGCAAGGTAGCGCACCTGTGGTCCCAGGTA
CTCAGGAGACTGAGGCATGAGAATCCCTTGAAACTGGGAGGCGGAAGTTGCAGTGAGCTG
TGATCGTGCCACTGCACTCCAGCCTGGTTGACAGAGCAACATGCTATCTCTAAAACAAAC
AAACAAACAAAAACTCAGGTTCCCACACCCTCTAAACCCTGCCTCCTCTCAGGCTACAGA
GACCTCTCCAGGAGGCTGAAGTGCCCTTACCCCGACCATCTGACCAGCCACCGCCCCATG
CCCGTGCCCCACCGAGGGCGGAGGCTGCTCACTGCTCTGTTTTATCTCTGGCCTCTGATC
CTGCATTCTTGTGCCAGGGCTTAGACCCAGGGCAAGGTCTTAGACCCAGGGCAGGGGTAG
GGTTAAAGGCTTTCAACCCAGGGGCCAGTGCCTTAATTCATGCAACAAATGTTTTCTGGC
TGTGTGCTTTATTCATGTGAACCAGGAAAACAGAAAAATATGACAGTGTTTCCAACAGAG
GTTTATAAGTGCTATGCAGGGCTGGTGGAAAGAGTAGAAACTGAGAAAGATAAACTTTAC
CCACTTGAAGGGAAGGAGGGCAATGTTACCAAGAAGGTAACATTTGAGTTGGGTCTTCAA
GGATGAATAGGAGTTCGGCATGCAAAGAGAGTTAGAAACCAACTTTTAGGAGTGGGGAGG
GGCTCTCATGTGCTACATACAATCTGAGGCACATTATATATGCCTAATCCCATTTTACAG
ATTAGAAAACTGGGGCTCAGAGGGTTAACTTGCCCACATTCACCTAACTGTAAATGGCAG
AGAAACAGGATTTCAAGTCCATGCCCATCCTATTGCCCCAGCATTCACAGAAAGCAGATG
GAGACATTCGTGTGTGAAGCACACAGGTATGAAAAGATGTACCAAGTTTGGTGTGGCTCA

AGTACATGGTACCTAAGGGAGTAGGTGAGAGAGAAAGCAGAAGAAAAAGACAGCAACAGG

**Figure S5.** The nucleotide sequences of 3′UTR of *TNS4* in A549 cells. Several variants of the 3′UTR of *TNS4* existed in A549 cells. The putative binding site of *miR-150-3p* was found in 3′UTR of *TNS4*, respectively (highlighted in blue). Red font was stop codon. There was no binding site of *miR-150-5p* in 3′UTR of *TNS4*.

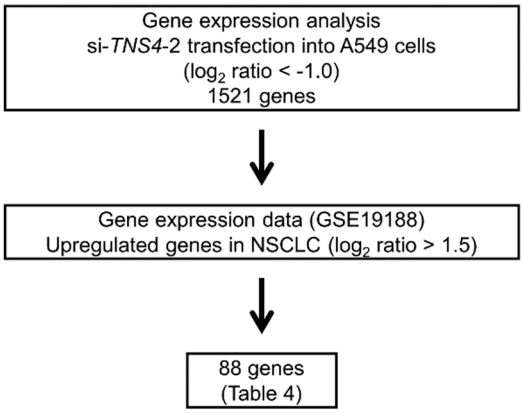


**Figure S6.** The strategy for identification of *TNS4*-modulated genes. We combined the gene expression analyses using A549 cells transfected with si-*TNS4* and GEO database (GSE19188). Finally, a total of 88 genes were identified as *TNS4*-modulated genes.

**Table S1.** Reagents used in this study.

| **Antibody** | **Dilution** | **Catalog Number** | **Company** |
|---|---|---|---|
| TNS4 | IHC 1:50<br>WB 1:500 | ab82178 | Abcam, Cambridge, UK |
| GAPDH | WB 1:20000 | MAB374 | EMD Millipore, Billerica, MA, USA |
| miRNA species | Concentration | Assay ID | Company |
| *miR-150-5p* | 10 nM | PM 10070 | Applied Biosystems, Foster City, CA, USA |
| *miR-150-3p* | 10 nM | PM 12324 | Applied Biosystems, Foster City, CA, USA |
| negative control miRNA | 10 nM | AM 17111 | Applied Biosystems, Foster City, CA, USA |
| anti-miR Negative Control #1 | 10 nM | AM 17010 | Applied Biosystems, Foster City, CA, USA |
| siRNA | Concentration | Catalog number | Company |
| si-*TNS4* | 10 nM | HSS131536<br>HSS131537 | Invitrogen, Carlsbad, CA, USA |
| Primer and probe | | Assay ID | Company |
| *miR-26a* | | 000405 | Applied Biosystems, Foster City, CA, USA |
| *miR-150-5p* | | 000473 | Applied Biosystems, Foster City, CA, USA |
| *miR-150-3p* | | 002637 | Applied Biosystems, Foster City, CA, USA |
| *RNU48* | | 001006 | Applied Biosystems, Foster City, CA, USA |
| *TNS4* | | Hs00262662_m1 | Applied Biosystems, Foster City, CA, USA |
| *GUSB* | | Hs00939627_m1 | Applied Biosystems, Foster City, CA, USA |
| Plasmid vector | | Catalog number | Company |

| | | |
|---|---|---|
| *TNS4* | RC222349 | OriGene Technologies Inc., Rockville, MD, USA |

**Table S2.** Immunohistochemical status and characteristics of the lung cancer and non-cancerous cases.

**A. Immunohistochemical status and characteristics of LUAD cases**

| Patient no. | Grade | T | N | M | Pathological stage | Immunohistochemical intensity | Immunohistochemical extensity |
|---|---|---|---|---|---|---|---|
| 21 | 1 | 1 | 0 | 0 | IA | 3 | 3 |
| 22 | 1 | 2 | 1 | 0 | IIA | 3 | 3 |
| 23 | 2 | 1 | 0 | 0 | I | 3 | 3 |
| 24 | 2 | 2 | 2 | 0 | IIIA | 2 | 3 |
| 25 | 2 | 3 | 1 | 0 | IIIA | 3 | 3 |
| 26 | 2 | 2 | 0 | 0 | IB | 3 | 3 |
| 27 | 2 | 3 | 2 | 0 | IIIA | 3 | 3 |
| 28 | 2 | 1 | 0 | 0 | IA | 2 | 3 |
| 29 | 2 | 3 | 1 | 0 | IIIA | 1 | 3 |
| 30 | - | 4 | 0 | 0 | IIIA | 3 | 3 |
| 31 | 2 | 2 | 0 | 0 | IIA | 1 | 3 |
| 32 | 2 | 3 | 1 | 0 | IIIA | 2 | 3 |
| 33 | 2 | 2 | 1 | 0 | IIB | 1 | 3 |
| 34 | 2 | 3 | 0 | 0 | IIB | 0 | 0 |
| 35 | 2 | 3 | 1 | 0 | IIIA | 2 | 3 |
| 36 | 3 | 2 | 1 | 0 | IIB | 3 | 3 |
| 37 | 3 | 2 | 0 | 0 | IB | 1 | 3 |
| 38 | 2 | 2 | 0 | 0 | IB | 1 | 3 |
| 39 | - | 2 | 0 | 0 | IB | 3 | 3 |
| 40 | 2 | 2 | 1 | 0 | IIB | 1 | 3 |

**B. Immunohistochemical status of non-cancerous cases**

| patient no. | Immunohistochemical intensity | Immunohistochemical extensity |
|---|---|---|
| 87 | 0 | 0 |
| 88 | 1 | 2 |
| 89 | 1 | 3 |
| 90 | 1 | 3 |
| 91 | 1 | 2 |
| 92 | 1 | 3 |
| 93 | 1 | 2 |
| 94 | 1 | 1 |
| 95 | 1 | 3 |
| 96 | 2 | 3 |
| 97 | 1 | 2 |

| | | |
|---|---|---|
| 98 | 1 | 3 |
| 99 | 2 | 3 |
| 100 | 2 | 2 |